universität wien

Ph.D. Thesis

Development and Optimization of Multifunctional Nanoparticles for Molecular Imaging

Submitted in fulfilment of the requirements for the degree

Doctor of Sciences (Dr. rer. nat.)

Vienna, 2009

Author: Dipl. Ing. Amitava Kundu

Matriculation number: 9403137

Doctoral subject: Chemistry (A091 419)

Supervisor: Univ. Prof. Dr. Dr. Bernhard K. Keppler

universität wien

DISSERTATION

Entwicklung und Optimierung multifunktioneller Nanopartikel für die molekulare Bildgebung

zur Erlangung des akademischen Grades

Doktor der Naturwissenschaften (Dr. rer. nat.)

Wien, 2009

Autor: Dipl. Ing. Amitava Kundu

Matrikel Nummer: 9403137

Dissertationsgebiet: Chemie (A091 419)

Betreuer: Univ. Prof. Dr. Dr. Bernhard K. Keppler

Acknowledgements

The work described in this thesis would not have been possible without help from many people.

First of all, I would like to thank Prof. Bernhard K. Keppler for offering the possibility to perform my Ph.D. thesis in his working group and providing financial support. I am also grateful for the interesting and challenging topic of my thesis and especially for pushing me forward to develop competences beyond chemical science.

I am grateful to Prof. Vladimir Arion for his support of my work and for the assistance in the preparation of this thesis.

I would like to thank my colleague Dr. Irena Paschkunova-Martic for good collaboration and the support at the beginning of my work even during her maternity leave.

I would like to thank Mag. Sergey Abramkin, Dr. Michael Reithofer, Dr. Florian Biba, Dr. Wolfgang Kandioller and Prof. Markus Galanski for recording NMR spectra and Dipl. Chem. Anna Bytzek for ICP-MS measurements.

I would like to thank my collaboration partners from other institutes: Prof. Herwig Peterlik from the Faculty of Physics for providing SAXS measurements, Mag[a]. Stephanie Ottofülling from the Department of Environmental Geosciences for particle size determinations and finally, Dr. Martin Krssak and Prof. Thomas Helbich from the Medical University of Vienna for performing MRI experiments.

I especially would like to thank Dr. Wolfgang Kandioller. His promotion is responsible for my choice to join Prof. Keppler´s group.

I want to express my gratitude to my parents Bimal and Christina Kundu for always supporting me and making all this possible.

I am deeply grateful to my beloved wife Klara for her ongoing love, her support in every aspect of my life and last but not least for the preparation of my every day lunch. I enjoyed it every single time.

Finally, I have to thank myself for being stubborn and consequent to pursue my aims even under difficult circumstances – never give up.

This thesis is based on the following manuscripts:

Novel active ester mediated functionalization and conjugation of Fmoc-Lysine and Polylysine to a bifunctional chelating ligand

Amitava Kundu, Bernhard K. Keppler

Strategies for the covalent conjugation of a bifunctional chelating agent to albumin: synthesis and characterization of potential MRI contrast agents

Amitava Kundu, Herwig Peterlik, Martin Krssak, Anna K. Bytzek, Thomas H. Helbich, Bernhard K. Keppler

Preparation of gadolinium chelate coated HSA-lectin nanoparticles for magnetic resonance imaging

Amitava Kundu, Stephanie Ottofuelling, Martin Krssak, Frank v.d. Kammer, Thilo Hofmann, Thomas H. Helbich, Bernhard K. Keppler

TABLE OF CONTENT

Abstract

In the field of medical diagnosis magnetic resonance imaging (MRI) has become a powerful tool. High spatial resolution and the capacity of differentiating soft tissue made MRI the most widespread imaging modality in clinical diagnosis. This technique is non invasive and therefore provides biomedical spectroscopy and spatial information without destroying the investigated sample. To increase the effectiveness of MRI and therefore enhance contrast between tissues paramagnetic contrast agents (CA) are applied. Though, these low molecular CA suffer from quick diffusion into the interstitium and rapid renal clearance. To overcome the mentioned limitations CA are coupled to nanosized carriers. This method promises prolonged intravascular retention leading to an increase in time, suitable for MRI measurements and due to prevented diffusion, an improved contrast.

In effort to develop improved nanosized MRI CA, this thesis focuses on the evaluation of different strategies for the conjugation of a bifunctional chelating ligand to a nanosized carrier protein. The methods developed in this work were evaluated according to the amount of attached bifunctional chelators, the shape and size dimension of the resulting particles and finally, their impact on magnetic relaxation.

In order to accumulate nanoshaped CA in the vasculature and visualize pathogenic alteration of blood vessels, the prepared CA were conjugated to an endothelial cell targeting lectin. These crosslinked nanoparticles were prepared in different sizes and lastly, MRI experiments were performed to determine relaxation.

Zusammenfassung

Magnetic Resonance Imaging (MRI) zählt heute zu den wichtigsten bildgebenden Verfahren in der medizinischen Diagnostik. Hohe räumliche Auflösung und die Fähigkeit zwischen verschieden Gewebearten zu unterscheiden, haben erheblich zur Verbreitung der Magnetresonanztomographie als Diagnoseinstrument beigetragen. Mit Hilfe dieser nicht invasiven Technik ist es möglich, exakte, biomedizinische Informationen zu erhalten, ohne die zu untersuchende Probe zu schädigen. Um die Leistung der Magnetresonanztomographie zu verbessern und die erhaltenen Signale zu verstärken, werden häufig paramagnetische Kontrastmittel eingesetzt. Diese niedermolekularen Substanzen weisen jedoch einen entscheidenden Nachteil auf: sie diffundieren rasch durch Poren in Blutgefäßen in angrenzendes Gewebe und werden schnell durch die Niere abgebaut und ausgeschieden. Eine vielversprechende Möglichkeit die Verweildauer in Blutgefäßen zu erhöhen ist, diese Kontrastmedien an makromolekulare Trägersubstanzen zu binden. Dadurch wird ein zu rasches Diffundieren verhindert und ein verlängerter Zeitrahmen für MRI Messungen, der verbesserte Abbildungen ermöglicht, steht zur Verfügung.

Im Bestreben, verbesserte Kontrastmittel im Nanometermaßstab zu entwickeln, zielt die vorliegende Arbeit auf die Entwicklung neuer Kopplungstechniken zwischen bifunktionellen Komplexbildnern und Trägerproteinen ab. Die daraus resultierenden modifizierten Proteine wurden auf den Gehalt anhängender Liganden, Größe und Struktur getestet. Anschließend gaben MRI Messungen über den Einfluss auf die Relaxivität, Auskunft.

Zusätzlich wurden diese nanopartikuären Kontrastmedien mit Lektinen gekoppelt, die an Endothelzellen binden. Damit soll eine noch längere Verweilzeit in Blutgefäßen

gewährleistet werden, was die Diagnose von krankhaften Veränderungen verbessert. Diese Lektinkonjugate wurden mithilfe unterschiedlicher Methoden in verschiedenen Größen hergestellt und ebenfalls ihr Einfluss auf das Relaxivitätsverhalten getestet.

Abbreviations

BFCA	bifunctional contrast agent
Bn	benzyl
BOPTA	3-benzyloxy-2-[(2-{[2-(biscarboxymethyl-amino)ethyl]carboxymethylamino}ethyl)carboxymethylamino]-propionic acid
BT-DO3A	1,4,7,10-tetraazacyclododecane-1-(2,3-dihydroxy-1-hydroxymethylpropyl)-4,7,10-trisacetic acid
CA	contrast agent
CT	computed tomography
Da	Dalton
DOTA	1,4,7,10-tetraazacyclododecane-*N,N′,N″,N‴*-tetraacetic acid
DTPA	diethylenetriaminepentaacetic acid
DTPA-BMA	DTPA-bismethylamide
DTPA-BMEA	DTPA-bismethoxyethylenamide
EOB-DTPA	{[2-(biscarboxymethylamino)-3-(4-ethoxyphenyl)propyl]-[2-(biscarboxymethylamino)ethyl]amino}acetic acid
ESI-MS	electrospray ionisation mass spectrometry
Fmoc	Fluorenylmethoxycarbonyl

HP-DO3A	1,4,7,10-tetraazacyclododecane-1-hydroxypropyl-4,7,10-trisacetic acid
HSA	human serum albumin
ICP-MS	inductively coupled plasma mass spectrometry
LEA	Lycopersicon esculentum agglutinin
MRI	magnetic resonance imaging
NMR	nuclear magnetic resonance
PET	positron emission tomography
pH	pondus Hydrogenii
SAXS	small angle X-ray scattering

Introduction

Introduction

The application of magnetic resonance imaging for the visualization of internal structures in humans was first described in 1977 (*1*). In the field of medical diagnosis and biomedical research magnetic resonance imaging (MRI) has become a versatile technique. High spatial resolution and the capacity of differentiating soft tissue made MRI the most widespread imaging modality in clinical diagnosis. This imaging technique is non invasive and therefore provides biomedical spectroscopy and spatial information without destroying the investigated sample. Generation of images by this method is based on the principles of nuclear magnetic resonance (NMR) – a well known tool for the characterization of chemical substances. The resonance of water protons combined with computational tools enables three dimensional visualization of the investigated biological structure. Beside MRI, several other medical imaging modalities are currently applied.

Radiography:

Radiography was the first and for a long period of time the only imaging modality available. Radiographs are generated by transmission of X-rays through the patient to a silver impregnated film. The contrast is produced by different scattering effects based on distinct tissue densities when X-rays pass the body and hit the impregnated film. It is still the first study ordered in evaluation of the lungs, heart and skeleton because of its wide availability, speed and relative low cost. A risk to health poses the

use of ionizing radiation. X-rays have the potential of causing genetic damage and cancer.

Fluoroscopy:

Fluoroscopy is used to obtain moving real time images of internal structures by employment of a fluoroscope. In the fluoroscope the patient is placed between an X-ray source and a fluorescent screen coupled to an X-ray image intensifier. Swallowed or injected contrast enhancing agents are used to investigate anatomy and functioning of the blood vessels, the genitourinary or the gastrointestinal tract. Radiocontrast agents like barium sulfate or iodine in different modifications strongly absorb or scatter X-ray radiation, and in conjunction with the real-time imaging provide insight to internal dynamic processes. Due to the use of X-ray, fluoroscopy poses a high potential risk to patients.

Computed Tomography (CT)

In CT, X-rays and computing algorithms generate three dimensional images of the examined body. An X-ray source together with an X-ray detector in the opposite are placed in a short tubular apparatus rotating around a patient and produce computer generated cross-sectional images (tomogram) in high spatial resolution. CT scans of internal organs, bones, soft tissue and blood vessels provide greater clarity and reveal more details than regular X-ray exams. Iodine-based contrast agents are considered as industry standard for CT but additionally, gadolinium-containing contrast agents have been used in place of iodinated contrast agents for certain

applications. Again the involvement of ionizing radiation causes concerns about the potential health risk. CT exposes the patient to more radiation than a radiograph.

Nuclear Medicine:

Nuclear medicine involves the administration of radioactive tracers coupled to substances with affinity for certain body tissues. Generally, radioactive isotopes of gallium, iodine and thallium are used as tracers. Nuclear medicine does not provide high spatial resolution images but it enables insight in the physiological function of the examined tissue. Produced images can be combined with simultaneously taken CT scans to improve the diagnostic accuracy.

A nuclear medicine technology using a radioactive biologically-active substance - most often fluorine-18 - is positron emission tomography (PET). Metabolically more active tissues like cancer concentrate the active fluorine-18 more than other tissues. The functional images provided by PET, displaying the spatial distribution of metabolic and biochemical processes, is often combined with high spatial resolution anatomical images from CT to increase precision of generated information.

Ultrasound:

Visualization of soft tissue structures in real time is provided by the utilization of ultrasound. This so called ultrasonography enables three dimensional imaging of fetal anatomic development as well as dynamic evaluation of the heart and major blood vessels. Limitations arise by the incapability to image through air (lungs) or bones. Compared to other diagnostic facilities the equipment for this technology is cheap

and is therefore one of the most widespread imaging modality in modern medicine. Ultrasonography does not use ionizing radiation and is hence, generally considered safe. Nevertheless, ultrasound enhances inflammatory response and it can heat soft tissue.

Beside the already mentioned non invasiveness, MRI displays another important advantage compared to the imaging techniques described above which has highly contributed to its widespread use. It does not expose the patient to harmful ionizing radiation. Furthermore, MRI scans give the best soft tissue contrast of all the imaging modalities (*2*, *3*, *4*, *5*).

Physical principles of MRI

Absorption and emission of energy in the radio frequency range of the electromagnetic spectrum is the base of MRI. Produced images derive from spatial variations in the phase and frequency of the radio frequency energy being absorbed and emitted by the imaged object. The human body mostly consists of water. Nuclei of hydrogen protons have a quantum mechanical property – the nuclear spin angular momentum. This is a vector (I) and can be quantified with the use of the Plank constant h.

$$|I| = \frac{h}{2\pi}\sqrt{I(I+1)}$$

For hydrogen the nuclear spin quantum number is ½. Placed in an external magnetic field (B_0), the hydrogen spin will precess about B_0 with the Larmor frequency (ω) in a discrete direction (Figure 1).

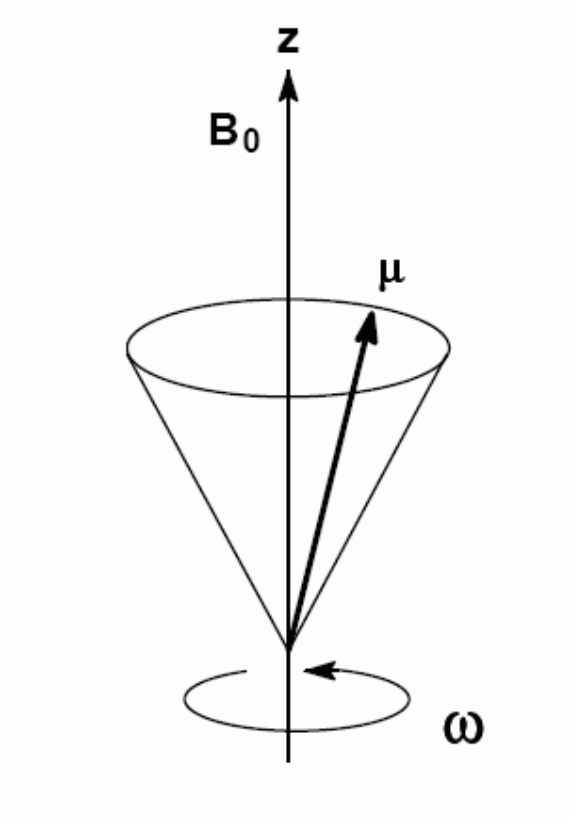

Figure 1 Precession of the magnetic moment μ about B_0 with the Larmor frequency ω

The spin of ½ enables two possible alignments corresponding to the energy level of the nucleus. Distribution of the spins between the two possible states is according to Boltzmann distribution, which is dependent on temperature T and the energy difference ΔE between the allowed states. The Boltzmann constant is represented by k.

$$\frac{N_{-1/2}}{N_{+1/2}} = \exp\left(-\frac{\Delta E}{kT}\right)$$

For hydrogen, the two energy states are $N_{+1/2}$ spin 'up' (low energy) and $N_{-1/2}$ spin 'down' state (high energy). The Boltzmann distribution shows that at 37℃, the average body temperature, slightly more spins occupy the lower energy state

generating the net magnetization vector M. These excess spins are used for the generation of the signal. The energy difference between the high and low energy states is proportional to the strength of the externally applied magnetic field B_0. The greater the strength of the external field, the greater the energy difference between the two spin states.

A second radiofrequency pulse which is perpendicular to B_0 can now be applied to generate field B_1. This field causes spins to flip off the z-axis and turn the net magnetization towards the transverse plane (x and y axis)

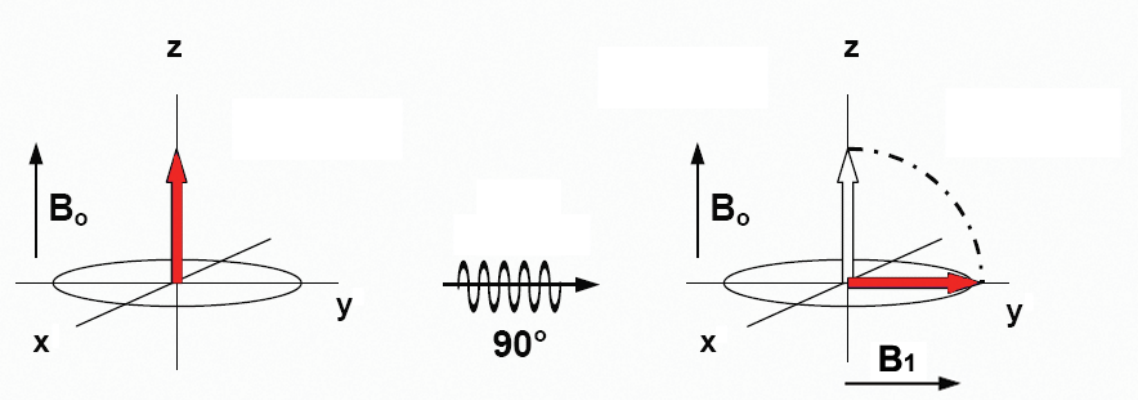

Figure 2 Application of a perpendicular radiofrequency pulse

The precessing about the *z*-axis in a xy-plane generates a detectable field. After the pulse, the generated B_1 ceases to exist and the nuclear spins return to their ground state. This process is called relaxation. The time required to return to the ground state is termed relaxation time. Relaxation time data of measured samples are used to produce the MR image.

Relaxation is considered in two parts: the recovery toward equilibrium alignment and the transverse decay. The return of the M alignment around the z-axis to equilibrium by a time constant is termed the spin-lattice relaxation T_1. Duration of the return from transverse decay is described as spin-spin relaxation T_2. These parameters provide MRI its power to distinguish between different tissues. T_1 and T_2 are properties of the water environment and thus of different tissue types. They differ between tissues due to the different physicochemical microenvironments of tissues like water mobility, the presence of microstructures, macromolecules and membranes (*2, 3, 4*).

Conrast agents in MRI

Spatial resolution in MRI is high. However, the potential of this diagnostic modality can be improved by the introduction of contrast agents (CA). MRI contrast agents are a class of pharmaceuticals that enhance the image contrast between tissues in which the agent accumulates and other tissues. This provides better differentiability of normal and diseased tissue and shows the status of organ function or blood flow (*6*). Nowadays, more than 35% of clinical MRI examinations are performed with the use of CA (*7*).

Types of CA

Currently availably CA for magnetic resonance can be divided into two groups: T_1 agents and T_2 agents. Generally, T_1 agents increase the spin-lattice relaxation rate ($1/T_1$) of hydrogen protons in tissue. This T_1 lowering effect increases the signal intensity on T_1 weighted images. T_1 agents have very little impact on the spin-spin relaxation. Due to the increase of signal intensity T_1 agents are called positive contrast agents. On the other hand, T_2 agents largely influence the spin-spin relaxation rate ($1/T_2$) by decrease of T_2. This results in the decrease of signal intensity on T_2 weighted images. Thus, these agents represent negative contrast agents (*8*) (Figure 3).

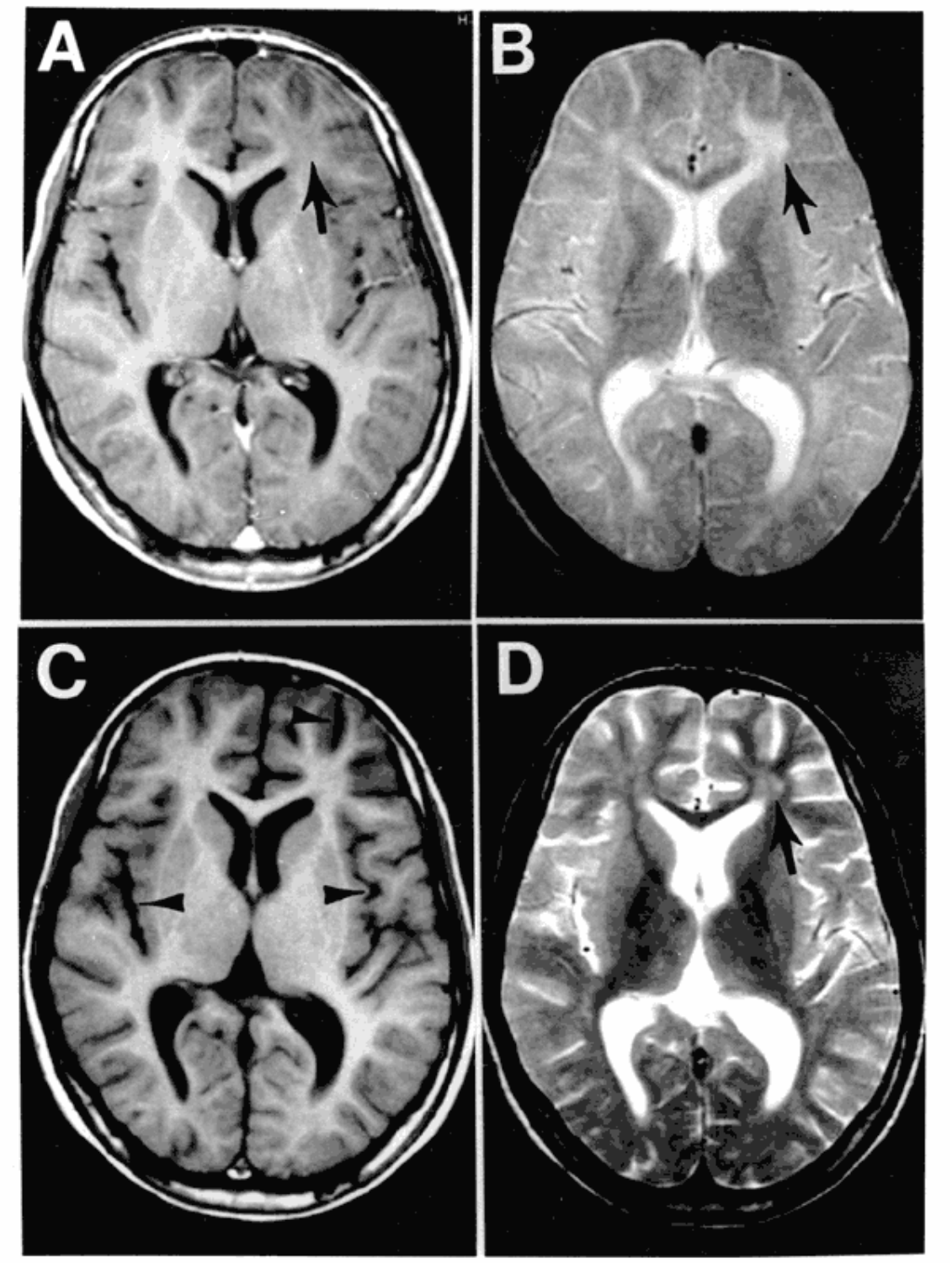

Figure 3. MRI scans of the brain. A and C are T_1 weighted images; B and D are T_2 weighted images. Picture taken from reference *9* with permission of the Centers for Disease Control and Prevention.

Due to their magnetic behavior, MRI CA can as well be described as superparamagnetic and paramagnetic agents.

Superparamagnetic contrast agents

Superparamagnetic contrast agents are water insoluble iron oxide crystals, usually based on magnetite (Fe_3O_4) or maghemite (γ-Fe_2O_3). Each iron oxide crystal consists of thousands of paramagnetic Fe ions (Fe^{2+} and Fe^{3+}), and if the Fe ions are magnetically aligned within the crystal, the net magnetic moment of the particle greatly exceeds that of typical paramagnetic ions. This effect is referred to as superparamagnetism and is characterized by a large magnetic moment in the presence of an external magnetic field (*10*).

Iron oxide CA are often coated by macromolecular materials including dextran, polysaccharide, chitosan, starch, albumin polystyrene and others. These contrast agents are commonly divided into three classes according to the mean total diameter. Below a size of 50 nm they are called ultra small superparamagnetic iron oxide (USPIO) particles. The term superparamagnetic iron oxide (SPIO) refers to particles where the mean diameter rises above 50 nm. And third, if the diameter is larger than 200 nm they are simply called large particles (*6*). Iron oxide agents do not leak into the interstitium and therefore they act as intravascular CA as long as the vessel endothelium is not altered by pathological processes.

The relaxation mechanism of these CA is referred to as susceptibility induced relaxation. Water molecules diffuse through the magnetic field gradients around the particles and the protons are relaxed by an outer sphere mechanism. The protons experience spin dephasing and transverse relaxation. As a consequence, T_2 is

shortened and the signal intensity on T_2 weighted images decreases. In addition to their effect on T_2, these agents also induce faster T_1 relaxation. Anyhow, they are commonly used as negative CA. The term outer sphere accounts for interactions between paramagnetic ions and closely diffusing water molecules, whereas inner sphere describes the relaxation of protons of water molecules directly bound to the CA.

Paramagnetic contrast agents

Paramagnetic CA are metal ions with unpaired electrons such as gadolinium (Gd^{3+}), manganese (Mn^{2+}, Mn^{3+}), iron (Fe^{2+}, Fe^{3+}), lanthanide (La^{3+}) and dysprosium (Dy^{3+}). All of them have already been used in MRI. Paramagnetic CA are shortening the relaxation time T_1 and induce therefore positive contrast.

By far, the most prominent type of paramagnetic CA consists of complexes with the Gd^{3+} ion. The ideal suitability of gadolinium results from a high magnetic moment given by seven unpaired f-electrons, the symmetric electronic state, high relaxivity and a coordination number of nine (Figure 4).

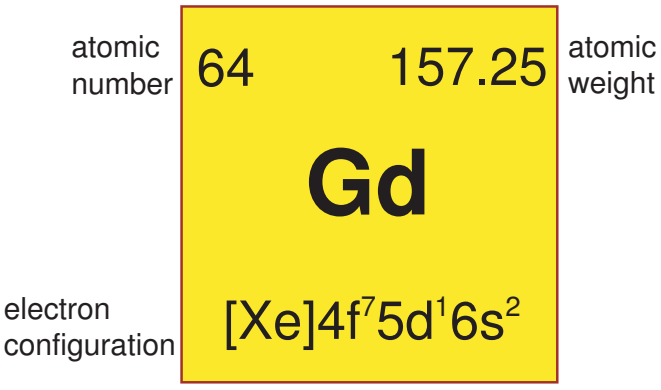

Figure 4. Electron configuration and atomic data of the rare earth metal gadolinium.

However, free heavy metal ions like Gd^{3+} are toxic and can not be applied in their ionic form. Damage to bone, spleen and liver occurs and furthermore free Gd^{3+} can cause nephrogenic systemic fibrosis (NSF) (*11*). For clinical use it must be bound in a complex to guarantee high stability and resistance towards transmetallation. The endogenous metal ions Zn^{2+} and Ca^{2+} are competitors and thus, the chelator has to exhibit higher complexation selectivity for Gd^{3+} than for Zn^{2+} and Ca^{2+}. To fulfil these requirements two types of polyaminocarboxylic acid derived ligands are employed. They are throughout based on the structural backbone of the linear diethylenetriaminepentaacetic acid (DTPA) or the macrocyclic 1,4,7,10-tetraazacyclododecane-*N,N',N'',N'''*-tetraacetic acid (DOTA) (*7*).

Gd chelates derived from these ligands have a coordination number of nine. Eight coordination sites are occupied by N and O of the multidentate ligands and one by a H_2O molecule, which is crucial for contrast enhancement (Figure 6).

The overall relaxivity is influenced by several physico-chemical parameters (*4*):

- the number of inner sphere water molecules directly bound to Gd^{3+}
- the residence time τ_m of the coordinated water molecule
- the rotational correlation time τ_r representing the molecular tumbling time of the complex (the slower the Gd^{3+} complex tumbles, the faster the relaxation rate)
- interaction of the complex with water molecules in the outer sphere
- electronic parameters

Figure 5 provides a schematic view on the interaction of Gd^{3+} with water molecules.

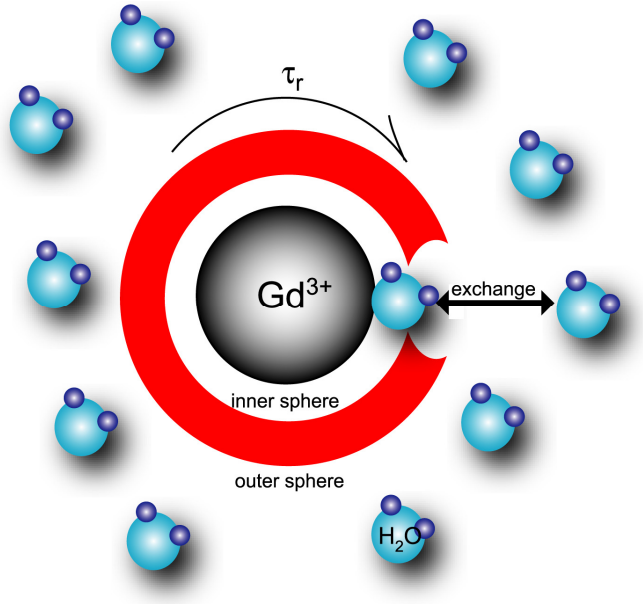

Figure 5. Interaction of Gd^{3+} with water molecules.

Low molecular weight contrast agents like Gd-DTPA (Magnevist®), Gd-DTPA-BMA (Omniscan®), Gd-DTPA-BMEA (OptiMARK®), Gd-BOPTA (MultiHance®), Gd-EOB-DTPA (Primovist®) and the cyclic Gd-DOTA (Dotarem®), Gd-HP-DO3A (ProHance®) and Gd-BT-DO3A (Gadovist®) are clinically approved and currently in use.

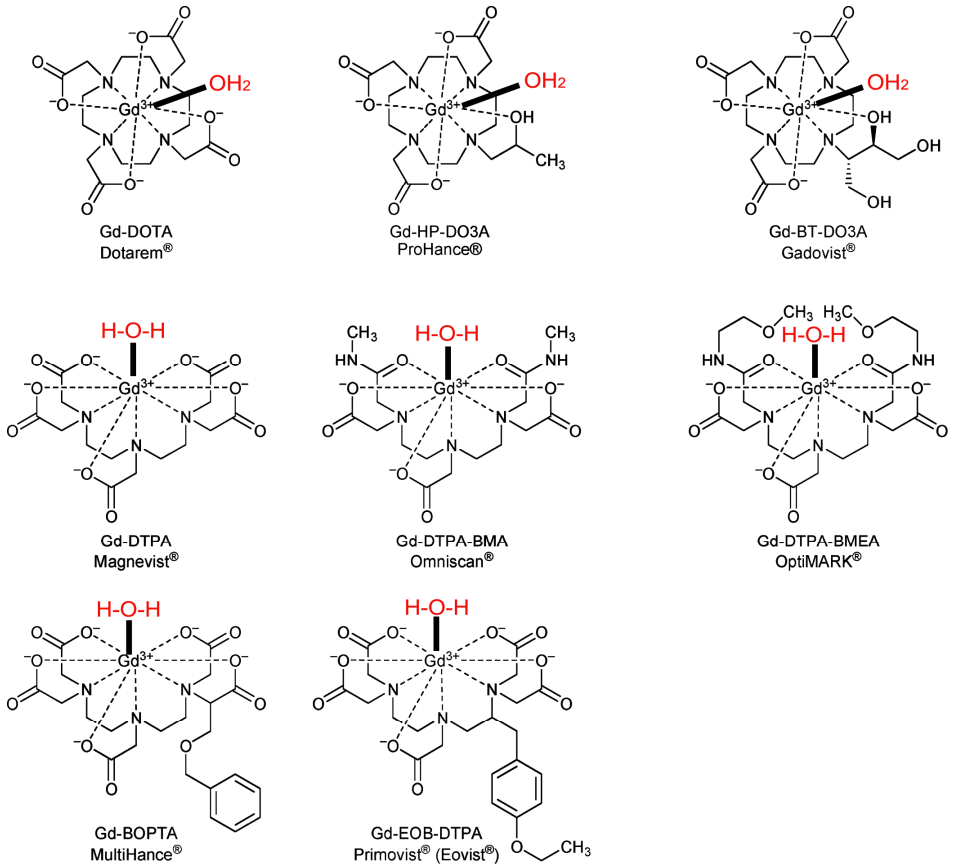

Figure 6. Clinically used low molecular weight contrast agents.

A rigorous drawback in the use of low molecular weight CA (mw < 1000 Da) is that they suffer from the disadvantage of diffusion from the vasculature into the interstitial space and rapid renal excretion (*12*).

Nanoparticles as CA for MRI

Contrast media in which numerous Gd(III) ions are covalently attached to a nanosphere are promising to overcome the limitations of low molecular weight agents. It is supposed that macromolecular contrast media (mw > 30000 Da) define a blood-tissue barrier comparable to the existing barrier for large molecular endogenous substances in the blood like plasma proteins and hematopoietic cells (*13*). These so called ´´Blood Pool Agents´´ are designed for prolonged intravascular retention and hence increasing molar relaxivities from the vasculature over an extended period of time.

Among a variety of nanosized carriers used for the attachment to gadolinium chelates, dextran is investigated due to its well established safety profile and biocompatibility. It can be synthesized to integrate a high density of gadolinium without intra-molecular cross-linking (*14*). Furthermore, it has a large number of hydroxyl groups suitable for additional conjugation to drugs.

Nanoparticles consisting of a polysaccharide backbone covalently derivatized with gadolinium complexing chelating ligands have also been studied and indicated enhanced T1 relaxivity (*15*).

Another type of macromolecular carrier are liposomes. They can be formed in different diameters varying from 20 - 400 nm with incorporated contrast enhancing substances. A rigorous drawback in the development of liposomes as nanosized contrast media is their polydispersity which hinders a reproducible synthesis (*12*).

The syntheses of polyethylene glycol attached lysine cascades nanosphere have also been reported and indicated strong, prolonged MRI enhancement of vessels (*16*).

Much attention has been paid to the possible application of dendrimers as nanospheres for macromolecular contrast agents (*12,17,18,19,20*). Dendrimers are highly branched synthetic polymers with a well defined structure, which can be prepared to specific sizes with reproducibility.

Gadolinium loaded albumins as macromolecular contrast agents have been investigated since 1987 when Gd-DTPA was covalently linked via amide formation to albumin molecules (*21*). The convenience of using serum proteins is based on their biocompatibility, stability and extended intravascular retention. Conjugations of Gd-DTPA or Gd-DOTA derivatives to albumin show high relaxivities and moreover, they are comparatively cheap and can easily be obtained (*12,22*).

A non covalent attachment of a DTPA derivative to human serum albumin is the strategy of MS 325 (*23,24*). This albumin targeted agent is specifically designed for blood vessel imaging. It is clinically approved and commercially available under the trademark Vasovist®. In this molecule, the DTPA backbone was modified by a phosphodiester linked biphenylcyclohexyl moiety (Figure 7). MS 325 binds reversibly human serum albumin in plasma.

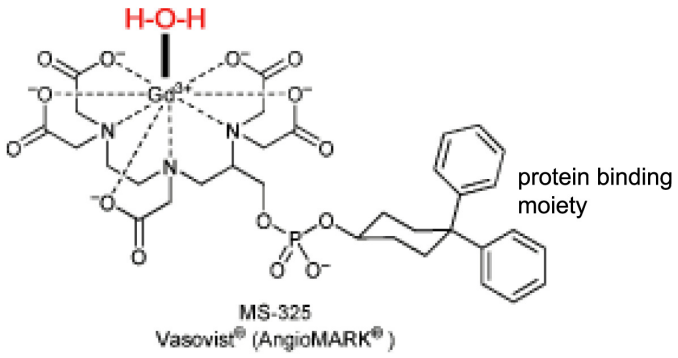

Figure 7. MS-325.

Bifunctional chelating agents

Attachment of the multidentate chelating DTPA or DOTA derived ligands to a nanosphere requires a functional group for conjugation. This functionality may not be involved in coordination to the Gd^{3+} ion and hence, destabilize the complex.

To avoid possible weakening of the gadolinium complexation that may lead to the release of free Gd^{3+} ions and cause undesirable side effects, a number of bifunctional chelating agents (BFCA) have been developed (*18,25,26*). Bifunctional chelators can bind tightly to the metal ion, while a further functionality acts as a linker to the macromolecule. In the case of MS 325 the additional functionality is the phosphodiester linked biphenylcyclohexyl moiety at the DTPA backbone (Figure 7). Although, it does not provide covalent conjugation, it enables binding to albumin without using the carboxylic acid functionalities which are necessary for metal coordination.

Another BFCA is 2-(*para*-aminobenzyl)-diethylenetriaminepentaacetic acid (NH_2-Bn-DTPA) which has an aminobenzyl residue attached (Figure 8). This residue is

suitable for the attachment to macromolecules. The coupling strategies to proteins of this BFCA will be discussed later in this thesis.

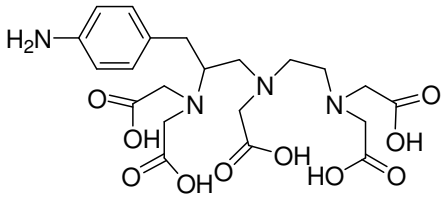

Figure 8. Bifunctional chelating agent NH_2-Bn-DTPA.

Targeting contrast agent

A remarkable perspective in MRI provides the introduction of a tissue specific targeting moiety to the contrast agent. High local concentration of contrast enhancing material at a particular site within the human body enables precise medical diagnosis and will become an essential tool in tracking the progress of therapies. Currently, great effort is invested in the development of such tissue specific contrast agents.

The concept of liver targeting is realized by the introduction of lipophilic moieties to the contrast agent or alternatively, the encapsulation of Gd-DTPA or Gd-DOTA chelates into liposomal nanoparticles (*27*).

Development of MRI contrast agents with the capability of seeking out tumors is approached by different strategies. One proposal is the non-covalent interaction of contrast agents bearing charged residues with charged groups of polyornithine and polyarginine. It is known, that positively charged polyaminoacids selectively bind to tumors as their charge is more negative than that of non-tumor cells (*28*). Receptor targeting through monoclonal antibodies attached to contrast enhancing molecules is also widely investigated in this field of research. Monoclonal antibodies are an important category of targeting vectors and can be prepared to interact with a variety

of receptor sites (*29*). Recently, the preparation and investigation of a peptide targeted contrast agent for molecular magnetic resonance imaging of fibronectin-fibrin complexes in tumor tissues was published (*30*).

The ability of imaging and diagnosing atherosclerotic plaques is of considerable interest since atherosclerotic diseases are among the leading causes of death in developed countries. Investigated methods to face the challenge of imaging fatty deposits include the application of recombinant high density lipoprotein (HDL) like nanoparticles (*31*). Newly published investigations provide characterization of plaque in deep seated arteries using motexafin gadolinium (*32*). MS 325, a gadolinium chelate that reversible binds to albumin in plasma has also been applied and areas of high signal intensity have been observed and were suggested not only to reflect the increased plaque vascularity but also the leakiness of the microvessels (*33*). In principle, also unspecific macromolecular or low molecular weight contrast agents suitable for imaging the blood pool bear the potential of indicating pathological alteration of the vasculature (*34*).

Lectins as target specific molecules

A group of biomolecules, with the capability to recognize specifically carbohydrate moieties of complex glycoconjugates and reversibly bind them are lectins. Lectins are non enzymatic glycoproteins usually of plant origin which possess carbohydrate recognition domains with specificities to various mono and oligosaccharides. The selectivity of lectins is determined by the exact shape of the binding site and the nature of amino acid residues to which the carbohydrate binds (*35*).

Recognition of carbohydrates on cell-surfaces by lectins has wide application in biological processes, including opsonization of microbes (enhancing phagocytes by coating a microbe), cell activation and differentiation, cell adhesion and migration, and apoptosis (*36*). Carbohydrate recognition by lectins often involves the side chains of tyrosine, tryptophan and histidine residues (*37*). Substitution of one or more amino acid residues leads to significant changes in lectin specificity. The carbohydrate is linked to the lectin by hydrogen bonds, van der Waals and hydrophobic interactions.

Purified lectins are routinely applied in the determination of human blood groups (A, B, AB or 0).

A targeting group capable of binding to endothelial cells is the tomato derived lectin LEA (Lycopersicon esculentum agglutinin) (*38,39*). Lectins connected to endothelial surfaces remain associated with the vascular wall for 2-3 h. Consequently, when LEA is conjugated to a CA, long MRI acquisition times and therefore high spatial resolution should be attainable (*40*). The ability of imaging blood vessels and prolonged intravascular retention of LEA conjugated gadolinium loaded latex nanoparticles has already been proven (*41*).

Scope of the thesis

Research in the field of magnetic resonance imaging contrast agents is an area of vast dimensions. The development of clinically applicable CA requires collaboration in multidisciplinary teams derived from sciences like chemistry, physics and medicine. Design, synthesis and evaluation of Gd^{3+} chelators as well as the choice of a suitable nanosphere and adequate linking strategies have to be investigated. The necessity of combination with tissue targeting molecules is a further demand which has to be fulfilled in order to face today challenges of increasing rates of cancer and atherosclerotic diseases. Finally, *in vivo* behavior and pharmacokinetic aspects have to be evaluated.

In an effort to develop improved nanosized MRI CA, the aim of this thesis focused on the evaluation of strategies for the conjugation of a bifunctional chelating ligand to a carrier protein. As described above, strong coordination of the contrast enhancing metal and additional coupling to carrier molecule is of great importance. For this purpose, a newly developed active ester was employed to link between the ε-amines of lysine and the BFCA (Figure 8). Due to good characterization possibilities, the reaction was developed and optimized by the employment of the test systems Fmoc-lysine and polylysine. Later, the method was adapted to modify human serum albumin (HSA).

In addition to the active ester strategy, further techniques to attach multiple BFCA to HSA, employing glutaric acid anhydride and glutaraldehyde, were investigated and subsequently, the relaxation behavior of the prepared CA was evaluated.

Furthermore, conjugation of the gadolinium modified albumins and the endothelial cell targeting LEA for the preparation of tissue specific nanoparticles was performed.

Several methods for the nanoparticle preparation in different sizes were evaluated and as well tested on their impact on relaxation.

References

(1) Hinshaw, W. S., Bottomley, P. A., Holland, G. N. (1977) Radiographic thin-section image of the human wrist by nuclear magnetic resonance. *Nature 270,* 722-723.

(2) Bohr, H. G. (2009) Handbook of molecular biophysics: Methods and applications. Wiley & Sons, Inc.

(3) S. Webb (1993) The Physics of Medical Imaging. Institute of Physics Publishing, Bristol; Philadelphia.

(4) Merbach, A. E., Tóth, É. (2001) The Chemistry of Contrast Agents in Medical Magnetic Resonance Imaging. John Wiley & Sons, New York.

(5) Burdette, J. (2008) In vivo imaging of molecular targets and their function in endocrinology. *Journal of Molecular Endocrinology 40*, 253–261

(6) Yan, G. P., Robinson, L., Hogg, P. (2007) Magnetic resonance imaging contrast agents: Overview and perspectives. *Radiography 13*, 5-19.

(7) Hermann, P., Kotek, J., Kubíček, V., Lukeš, I. (2008) Gadolinium (III) complexes as MRI contrast agents: ligand design and properties of the complexes. *Dalton Trans*. 3027-3047.

(8) Lauffer, R.B. (1996) MRI contrast agents: basic principles. *Clinical magnetic resonance imaging*. (Edelman, R. R., Hesselink, J. R., Zlatkin, M. B., Eds.) pp 176-191, 2nd ed. Pennsylvania: W.B. Saunders Company.

(9) Bonthius, D. J., Stanek, N., Grose, C. (2000) Subacute Sclerosing Panencephalitis, a Measles Complication, in an Internationally Adopted Child. *Emerging Infectious Diseases 6,* 377-381.

(10) Bjørnerud, A., Johansson, L. (2004) The utility of superparamagnetic contrast agents in MRI: theoretical consideration and applications in the cardiovascular system. *NMR Biomed. 17,* 465-477.

(11) Sieber, M.A., Pietsch, H., Walter, J., Haider, W., Frenzel, T:, Weinmann, H. J. (2008) A Preclinical Study to Investigate the Development of Nephrogenic Systemic Fibrosis: A Possible Role for Gadolinium-Based Contrast Media. *Invest. Radiol. 43*, 65-75.

(12) Barrett, T., Kobayashi, H., Brechbiel, M., Choyke, P. L. (2006) Macromolecular MRI contrast agents for imaging of tumor angiogenesis. *Eur. J. Radiol. 60,* 353-356.

(13) Brasch, R. C., Daldrup-Link, H. E. (2003) Macromolecular contrast agents for MR mammography: current status. *Eur. Radiol. 13*, 354-365.

(14) Sirlin, C. B., Vera, D. R., Corbeil, J. A., Caballero, M. B., Buxton, R. B., Mattrey, R. F. (2004) Gadolinium-DTPA-dextran: a macromolecular MR blood pool contrast agent. *Acad. Radiol. 11*, 1361-1369.

(15) Helbich, T. H., Gossman, A., Mareski, P. A., Radüchel, B., Roberts, T. P. L., Shames, D. M., Mühler, M., Turetschek, K., Brasch, R. C. (2000) A New Polysaccharide Macromolecular Contrast Agent for MR Imaging: Biodistribution and Imaging Characteristics. *J. Magn. Reson. Imaging 11*, 694-701

(16) Fu, Y., Raatschen, H. J., Nitecki, D. E., Wendland, M. F., Novikov, V., Fournier, L. S., Cyran, C., Rogut, V., Shames, D. M., Brasch, C. R. (2007) Cascade Polymeric MRI Contrast Media Derived from Poly(ethylene glycol) Cores: Initial Syntheses and Characterizations. *Biomacromolecules 8*, 1519-1529.

(17) Xu, H., Regino, C. A. S., Koyama, Y., Hama, Y., Gunn, A. J., Bernardo, M., Kobayashi, H., Choyke, P. L., Brechbiel, M. W. (2007) Preparation and preliminary evaluation of a biotin-targeted, lectin-targeted dendrimer-based probe for dual modality magnetic resonance and fluorescence imaging. *Bioconjugate Chem. 18*, 1474–1482.

(18) Kido, N., Xu, H., Regino, C. A. S., Bernardo, M., Ileva, L., Riffle, L., Wong, K. J., Brechbiel, M. W. (2009) A New Approach in the Preparation of Dendrimer-Based Bifunctional Diethylenetriaminepentaacetic Acid MR Contrast Agent Derivatives. *Bioconjugate Chem. 20*, 1412-1418.

(19) Xu, H., Regino, C. A. S., Bernardo, M., Koyama, Y., Kobayashi, H., Choyke, P. L., Brechbiel, M. W. (2007) Towards Improved Syntheses of Dendrimer-Based Magnetic Resonance Imaging Contrast Agents: New Bifunctional Diethylenetriaminepentaacetic Acid Ligands and Nonaqueous Conjugation Chemistry. *J. Med. Chem. 50*, 3185-3193.

(20) Langereis, S., de Lussanet, Q. G., van Genderen, M. H., Meijer, E. W., Beets-Tan, R. G., Griffioen, A. W., van Engelshoven, J. M., Backes, W. H. (2006) Evaluation of Gd (III) DTPA-terminated poly(propylene imine) dendrimers as contrast agents for MR imaging. *NMR Biomed. 19*, 133-141.

(21) Ogan, M. D., Schmiedl, U., Moseley, M. E., Grodd, W., Paanjanen, H., Brasch, R. C. (1987) Albumin labeled with Gd-DTPA. An intravascular contrast enhancing agent for magnetic resonance blood pool imaging: preparation and characterization. *Invest. Radiol. 22*, 665-671.

(22) Yan, G. P., Robinson, L., Hogg, P. (2007) Magnetic resonance imaging contrast agents: Overview and perspectives. *Radiography 13*, 5-19.

(23) Caravan, P., Parigi, G., Chasse, J. M., Cloutier, N. J., Ellison J. J., Lauffer, R. B., Luchinat, C., McDermid, S. A., Spiller, M., McMurry, T. J. (2007) Albumin Binding, Relaxivity, and Water Exchange Kinetics of the Diastereoisomers of MS-325, a Gadolinium(III)-Based Magnetic Resonance Angiography Contrast Agent. *Inorg. Chem. 46*, 6632-6639.

(24) Caravan, P. (2009) Protein-Targeted Gadolinium-Based Magnetic Resonance Imaging (MRI) Contrast Agents: Design and Mechanism of Action. *Acc. Chem. Res.42*, 851-862.

(25) Gugliotta, G., Botta, M., Giovenzana, G. B., Tei, L. (2009) Fast and easy access to efficient bifunctional chelators for MRI applications. *Bioorg. Med. Chem. Lett. 19*, 3442–3444.

(26) Chong, H. S., Ma, X., Le, T., Kwamena, B., Milenic, D. E., Brady, E. D., Song, H. A., Brechbiel, M. W. (2008) Rational Design and Generation of a Bimodal Bifunctional Ligand for Antibody-Targeted Radiaton Cancer Therapy. *J. Med. Chem. 51,* 118-125.

(27) Weinmann, H. J., Ebert, W., Misselwitz, B., Schmitt-Willich, H. (2003) Tissue-specific MRI contrast agents. *Eur. J. Radiol., 46*, 33-44.

(28) Aime, S., Botta, M., Garino, E., Crich, S. G., Giovenzana, G., Pagliarin, R., Palmisano, G., Sisti, M. (2000) Non-covalent Conjugates between Cationic Polyamino Acids and Gd (III) Chelates: A Route for Seeking Accumulation of MRI-Contrast Agents at Tumor Targeting Sites. *Chem. Eur. J., 6*, 2609-2617.

(29) Jaques, V., Desreux, J. F. (2002) New Classes of MRI Contrast Agents. *Topics In Current Chemistry, 221,* 123.164.

(30) Ye, F., Jeong, E. K., Jia, Z., Yang, T., Parker, D., Lu, Z. R. (2008) A Peptide Targeted Contrast Agent Specific to Fibrin-Fibronectin Complexes for Cancer Molecular Imaging with MRI. *Bioconjugate Chem., 19,* 2300-2303.

(31) Frias, J. C., Williams, K. J., Fisher, E. A., Fayad, Z. A. (2004) Recombinant HDL-Like Nanoparticles: A Specific Contrast Agent for MRI of Atherosclerotic Plaques. *J. Am. Chem. Soc., 126,* 16316-16317.

(32) Brushett, C., Qiu, B., Atalar, E., Yang, X. (2008) High Resolution MRI of Deep Seated Atherosclerotic Arteries Using Motexafin Gadolinium. *J. Magn. Reson. Imaging, 27,* 246-250.

(33) Choudhury, R. P., Fuster, V., Badimon, J. J., Fisher, E. A., Fayad, Z. A. (2002) MRI and Characterization of Atherosclerotic Plaque: Emerging Applications and Molecular Imaging. *Arterioscler. Thromb. Vasc. Biol., 22,* 1065-1074.

(34) Briley-Saebo, K. C., Mulder, W. J. M., Mani, V., Hyafil, F., Amirbekian, V., Aguinaldo, J. G. S., Fisher, E. A., Fayad, Z. A. (2007) Magnetic Resonance Imaging of Vulnerable Atherosclerotic Plaques: Current Imaging Strategies and Molecular Imaging Probes. *J. Magn. Reson. Imaging, 26,* 460-479.

(35) Sharon N., Lis H. (1995) Lectins-proteins with a sweet tooth: functions in cell recognition.

Essays Biochem. 30, 59-75.

(36) Sharma V., Surolia A. (1997) Analyses of carbohydrate recognition by legume lectins: size of the combining site loops and their primary specificity. *J. Mol. Biol. 267*, 433-445.

(37) Siebert H.C., von der Lieth C.W., Kaptein R., Beintema J.J., Dijkstra K., van Nuland N., Soedjanaatmadja U.M., Rice A., Vliegenthart J.F., Wright C.S., Gabius H.J. (1997) Role of aromatic amino acids in carbohydrate binding of plant lectins: laser photo chemically induced dynamic nuclear polarization study of hevein domain-containing lectins. *Proteins 28*, 268-284.

(38) Porter, G. A., Palade, G. E., Milici, A. J. (1990) Differential binding of the lectins Griffonia simplicifolia I and Lycopersicon esculentum to microvascular endothelium: organ-specific localization and partial glycoprotein characterization. *Eur. J. Cell Biol. 51,* 85-95.

(39) Mazzetti, S., Frigerio, S., Gelati, M., Salmaggi, A., Vitellaro-Zuccarello, L. (2004) Lycopersicon esculentum lectin: an effective and versatile endothelial marker of normal and tumoral blood vessels in the central nervous system. *Eur. J. Histochem. 48*, 423-428.

(40) Debbage P.L., Seidl S., Kreczy A., Hutzler P., Pavelka M., Lukas P. (2000) Vascular permeability and hyperpermeability in a murine adenocarcinoma after fractionated radiotherapy: an ultrastructural tracer study. *Histochem Cell Biol 114,* 259-275.

(41) Paschkunova-Martic, I., Kremser, C., Mistlberger, K., Shcherbakova, N., Dietrich, H., Talasz, H., Zou, Y., Hugl, B., Galanski, M., Sölder E., Pfaller, K., Höliner, I., Buchberger, W., Keppler, B., Debbage, P. (2005) Design, synthesis, physical and chemical characterisation, and biological interactions of lectin-targeted latex nanoparticles bearing Gd-DTPA chelates: an exploration of magnetic resonance molecular imaging (MRMI). *Histochem. Cell. Biol. 123,* 283-301.

Novel active ester mediated functionalization and conjugation of Fmoc-Lysine and Polylysine to a bifunctional chelating ligand

Amitava Kundu, Bernhard K. Keppler

Institute of Inorganic Chemistry, University of Vienna

Abstract

Lysine is an important moiety of macromolecules with the capability of convenient modification. Attachment of ligands to these amino acids is a crucial step in the development of protein or peptide based diagnostic facilities. Here, a new active ester mediated methodology is described which enables functionalization of the *ε*-amines of Fmoc lysine and poly-*L*-lysine by the covalent coupling to a bifunctional chelating agent. Bromoacetylation of lysine and subsequent n-alkylation of the primary amine functionality of the bifunctional chelating agent were performed in moderate to good yields. The synthesized compounds were reliably characterized by NMR.

Introduction

Due to high spatial resolution and the capacity of differentiating soft tissues magnetic resonance imaging (MRI) has become the most widespread imaging modality. Based on its most prominent advantage - non invasiveness – MRI today is routinely applied for the visualization of internal structures. In clinical diagnosis and biomedical research information from three dimensions can easily be obtained without damaging tissue or the investigated sample. Furthermore, no exposure to potentially harmful ionizing radiation occurs. The potential of MRI can be increased by the application of contrast enhancing agents. Currently, Gd(III) chelates are the most frequently used MRI contrast agents (*1,2*). Among all known elements gadolinium exhibits the strongest effect on the longitudinal relaxation time. Though, free Gd(III) is toxic and the choice of a proper ligand is essential to prevent dissociation of the complex (*3*).

Gadolinium chelating ligands of clinically approved contrast agents (CA) are throughout based on the structural backbone of the linear diethylenetriaminepentaacetic acid (DTPA) or the macrocyclic 1,4,7,10-tetraazacyclododecane-N,N',N'',N'''-tetraacetic acid (DOTA). Such polyaminocarboxylic acid derived paramagnetic chelates like Gd-DTPA (Magnevist®), Gd-DTPA-BMA (Omniscan®), Gd-DTPA-BMEA (OptiMARK®), Gd-BOPTA (MultiHance®), Gd-EOB-DTPA (Primovist®) and the cyclic Gd-DOTA (Dotarem®), Gd-HP-DO3A (ProHance®) and Gd BT-DO3A (Gadovist®) are currently in use (*4*). Nevertheless, these low molecular weight agents suffer from the inconvenience of diffusion from the vasculature into the interstitial space and rapid renal excretion (*5*).

The concept of attaching Gd(III) chelates to nanospheres presents promising options for improved biophysical and pharmacological properties. Increased rotational correlation time for enhanced relaxivity per gadolinium atom and the prolonged intravascular retention provide the main advantages. Such macromolecular contrast media may define a blood-tissue barrier comparable to the existing barrier for large molecular endogenous substances in the blood like plasma proteins (*6*).

Among many macromolecular carriers for the preparation of contrast enhancing nanoparticles dextran is investigated due to its well established safety profile and biocompatibility. It can be synthesized to integrate a high density of gadolinium without intramolecular cross-linking (*7*). Liposomes are a different type of nanosized carrier and can be formed in different diameters for the incorporation of Gd(III) chelates (*5*). Much attention has also been paid to the potential application of dendrimers as nanospheres for macromolecular contrast agents (*5, 8, 9, 10, 11*). Dendrimers are highly branched synthetic polymers with a well defined structure and can be produced to specific sizes with reproducibility. A further important class of nanoparticular contrast agents are gadolinium loaded albumins. They have been investigated since 1987 when Gd-DTPA was covalently linked via amide formation to albumin molecules (*12*). The convenience of using serum proteins is based on their biocompatibility, stability and extended intravascular retention. Research also covered investigation in paramagnetically labelled polylysine (*13*,*14*). Gd(III) chelates covalently conjugated to polylysine have been extensively tested in order to find the optimal preparation for blood pool imaging (*15*). Additionally, grafted co-polymeric nanoparticles derived from polyethyleneglycol and polylysine cascades loaded with Gd-DTPA have been examined and showed prolonged MRI enhancement of blood vessels (*16*).

To prevent the relaese of free Gd(III) by a possible weakening of the gadolinium complex while attached to a nanosphere a number of bifunctional chelating agents (BFCA) have been developed (*10, 17, 18*). Bifunctional ligands can bind tightly to the metal ion while a further functionality acts as a linker to the macromolecule.

The importance of modifying lysine is shown by the versatile applicability of its polymer by the given examples from literature and by the fact that carrier proteins like serum albumins contain several lysine moieties capable for the conjugation with gadolinium chelating molecules like DTPA or bifunctional derivatives thereof. Furthermore, the adaptation of lysine residues plays a crucial role in the adjustment of antibodies for the purpose of targeted diagnosis and targeted drug delivery. In this study an active ester mediated coupling strategy for the conjugation of Fmoc-lysine or polylysine to a bifunctional chelating agent is presented. Development of a test system and the following application of the method to the bifunctional chelating agent are also reported. The activation of lysine at the terminating *ε*-amine was followed by conjugation to the primary amine functionality of the bifunctional chelating agent.

Experimental Section

Materials and Methods. Bromoacetic acid, *N,N*-diisopropylethylamine (DIPEA) and polylysine hydrobromide (mw: 15000 - 30000) were purchased from Sigma-Aldrich (Germany). 2,3,5,6-tetrafluorophenol, dimethylformamide (DMF, extra dry) and sodium iodide were obtained from Acros (Belgium). *N,N´*-dicyclohexylcarbodiimide (DCC), 4-aminobenzoic acid and Fmoc-*L*-lysine hydrochloride were purchased from Fluka (Germany). 2,6-Dimethylpyridine (lutidin) was received from Merck (Germany).

2-(*para*-Aminobenzyl)-diethylenetriaminepentaacetic acid tetrahydrochloride (*p*-NH_2-Bn-DTPA•4 HCl) was prepared according to literature procedures (*19*). All other solvents were obtained from different commercial suppliers and distilled prior use. For column chromatography, silica gel 60 from Fluka was used. NMR spectra were recorded at 24 °C on a Bruker Avance DPX 400 spectrometer (Ultrashield magnet) at 400.13 MHz (^{1}H) and 100.63 MHz (^{13}C). Elemental analyses were carried out with a Perkin-Elmer 2400 CHN elemental analyzer or by titration with an automatic titration system using 0.1 M $AgNO_3$ (DL 21, Mettler-Toledo, 1990) after Schöniger-decomposition (for Br), respectively at the Microanalytical Laboratory of the University of Vienna.

Bromoacetic acid, 2,3,5,6-tetrafluorophenylester (**1**). Bromoacetic acid (1.13 g, 8.15 mmol) and 2,3,5,6-tetrafluorophenol (1.36 g, 8.20 mmol) were dissolved in 30 ml CH_2Cl_2 and cooled to 0°C. A small amount of molecular sieve (3 Å) was added. DCC (1.88 g, 9.12 mmol) was dissolved in dichloromethane (15 ml) and added slowly to the reaction mixture. The reaction mixture was stirred at 0°C for 45 min. Then, the cooling bath was removed and the reaction mixture was allowed to stir further 45 min. at ambient temperature. Thereafter, the organic layer was extracted four times with water, dried over anhydrous Na_2SO_4 and evaporated under reduced pressure. Finally, the product was purified by Kugelrohr distillation (1.2×10^{-1} mbar, 63°C) to yield the product 1.95 g (6.80 mmol, 83%) as colorless oil.

^{1}H NMR ($CDCl_3$): δ= 4.14 (s, 2H), 7.04 (m, 1H); ^{13}C NMR ($CDCl_3$): δ= 23.7 (CH_2), 104.1 (t, CH, Ar), 129.3 (C, Ar), 139.6 – 141.7 (m, CF, Ar), 145.2 – 147.3 (m, CF, Ar), 163.6 (CO); Elemental analyses: calcd for $C_8H_3BrF_4O_2$ (M_w= 287.00) : C, 33.48; H, 1.05; Br, 27.84. Found: C, 33.50; H, 0.95; Br, 28.39.

6-(2-Bromo-acetylamino)-2-(9H-fluoren-9-ylmethoxycarbonylamino)-hexanoic acid (**2**). Fmoc protected lysine hydrochloride (0.10 g, 0.25 mmol) was dissolved in dry DMF under an Ar atmosphere. The solution was cooled to 0°C and DIPEA (0.1 ml, 0.547 mmol) was added slowly via syringe. Thereafter, the reaction mixture was stirred for 40 min. Bromoacetic acid, tetrafluorophenyl ester (**1**) (76 mg, 0.26 mmol) was dissolved in DMF (1 ml) and then added dropwise during 15 min. to the reaction mixture. Afterwards, the solution was stirred for 2 h at 0°C and one additional hour at ambient temperature. Finally, the solvent was evaporated at 60°C under reduced pressure. The product was purified by column chromatography ($CHCl_3$:CH_3:NH_3; 12:4:1; Rf: 0.3) and yielded **2** (0.73 g, 61%).

MS (ESI^-) *m/z* 488.8 $[M-H]^-$; ^1H NMR (DMSO-d_6): δ = 1.31 (m; 2H, CH_2-C<u>H</u>$_2$-CH_2), 1.39 (m; 2H, CH_2-C<u>H</u>$_2$-CH_2), 1.59 - 1.68 (m; 2H, CH-C<u>H</u>$_2$-CH_2), 3.06 (m; 2H, NH-C<u>H</u>$_2$-CH_2), 3.86 (m, 1H, NH-C<u>H</u>-COOH), 4.01 (s, 2H, CH_2Br), 4.20 - 4.30 (m; 3H,CH-CH_2-O), 7.33 (dd; 2H Ar-H, J= 7.5 Hz), 7.41 (dd; 2H, Ar-H, J= 7.5 Hz), 7.47 (s; 1H, NH), 7.72 (d; 2H, Ar-H, J= 7.9 Hz), 7.89 (d; 2H, Ar-H, J= 7.9 Hz), 8.21 (bs; 1H, NH). ^{13}C NMR (DMSO-d_6): δ = 22.9 (CH_2-<u>C</u>H_2-CH_2), 28.5 (<u>C</u>H_2Br), 29.8 (<u>C</u>H_2-CH_2-NH), 31.5 (CH_2-<u>C</u>H_2-CH-COOH), 42.7 (<u>C</u>H_2-NH), 46.9 (<u>C</u>H-CH_2-O), 54.4 (NH-<u>C</u>H-COOH), 65.5 (CH-<u>C</u>H_2-O), 120.1 (Ar-<u>C</u>H), 125.3 (Ar-<u>C</u>H), 127.1 (Ar-<u>C</u>H), 127.6 (Ar-<u>C</u>H), 140.7 (Ar-<u>C</u>), 143.8 (Ar-<u>C</u>), 155.9 (NH-COO), 165.8 (COOH), 173.9 (NH-<u>C</u>O-CH_2).

2-(9H-fluoren-9-ylmethoxycarbonylamino)-6-[2-(4-hydroxycarbonylphenyl) acetylamino)]-hexanoic acid (**3**). *para*-Aminobenzoic acid (10 mg, 0.06 mmol) and NaI (13 mg, 0.09 mmol) were suspended in dry DMF (1 ml) and cooled to 0°C. DIPEA (0.04 ml, 0.23 mmol) was added and the reaction mixture was stirred for 10 min. Bromoacetylated Fmoc-lysine (**2**) (22 mg, 0.04 mmol) was dissolved in DMF (0.5 ml) and added slowly to the reaction mixture. Afterwards, the reaction was allowed to proceed for 4 h at 0°C. Then, the cooling bath was removed and stirring continued for 21 h at room temperature. The solvent was removed at 60°C under reduced pressure and the product was separated from excess reagents by column chromatograpy ($CHCl_3$:CH_3:NH_3; 12:4:1; Rf: 0.1) to give **3** (21 mg, 88%).

MS (ESI^+) *m/z* 546.4 $[M+H]^+$; ^1H NMR (DMSO-d_6): δ = 1.22 (m; 2H, CH_2-C$\underline{H_2}$-CH_2), 1.35 (m; 2H, CH_2-C$\underline{H_2}$-CH_2), 1.56 (m; 1H, CH-C$\underline{H_2}$-CH_2), 1.67 (m; 2H, CH-C$\underline{H_2}$-CH_2), 3.04 ((m; 2H, NH-C$\underline{H_2}$-CH_2), 3.66 (m, 3H, NH-C$\underline{H}$-COOH; NH-CH_2-CO), 4.21-4.25 (m, 3H, CH-CH_2-O), 6.53 (d, 2H, Ar´-H, J= 8.5 Hz), 7.31 (m, 2H, Ar-H), 7.40 (m, 2H, Ar-H), 7.66 (m, 4H, Ar-H;Ar´-H), 7.88 (d, 2H, Ar-H, J= 7.5 Hz), 7.89 (bs; 1H, NH). ^{13}C NMR (DMSO-d_6): δ = 22.4 (CH_2-$\underline{C}H_2$-CH_2), 30.7 ($\underline{C}H_2$-CH_2-NH), 31.2 (CH_2-$\underline{C}H_2$-CH-COOH), 38.3 (CH_2-$\underline{C}$H2-NH), 46.3 (CO-$\underline{C}H_2$-NH), 54.0 (NH-$\underline{C}$H-COOH), 111.2 (Ar´-$\underline{C}$H), 117.9 (Ar´-$\underline{C}$-COOH), 120.1 (Ar-$\underline{C}$H), 121.4 (Ar-$\underline{C}$H), 127.3 (Ar-$\underline{C}$H), 128,9 (Ar-$\underline{C}$H), 130.8 (Ar´-$\underline{C}$H), 131.1 (Ar-$\underline{C}$H), 137.4 (Ar-$\underline{C}$), 139.4 (Ar-$\underline{C}$), 142.6 (Ar´-$\underline{C}$), 151.7 (NH-COO), 152.8 (Ar-$\underline{C}$OOH), 167,8 (NH-$\underline{C}$O-CH_2), 169.4 ($\underline{C}$OOH).

*Preparation of **4** by coupling of the BFCA to the* bromoacetylated *Fmoc-Lysine (**2**)*. *p*-NH_2-Bn-DTPA•4 HCl (21 mg, 0.03 mmol) and NaI (9 mg, 0.06 mmol) were dissolved in dry DMF (1 ml) and cooled to 0°C. DIPEA (0.05 ml, 0.29 mmol) was added and the

reaction solution was stirred for 20 min. Then, bromoacetylated Fmoc-lysine (**2**) (15 mg, 0.03 mmol) was dissolved in DMF (0.5 ml) and dropped during 30 min. to the reaction mixture. Thereafter, the reaction was allowed to stir for 20 h at 0°C. The solvent was evaporated under reduced pressure at 50°C to give the product **4**.

MS (ESI^-) *m/z* 905.9 $[M\text{-}OH]^-$

*Preparation of **5** by the bromoacetylation of polylysine hydrobromide*. Under an atmosphere of argon polylysine hydrobromide (35 mg) was suspended in a mixture of DMF (4 ml) and 2,6-dimethylpyridine (lutidine) (1 ml). The suspension was cooled to 0°C and active ester **1** (184 mg, 0.64 mmol) dissolved in DMF (1 ml) was added during 20 min. The suspension was stirred for 18 h. The resulting clear solution was added dropwise to a 1:1 mixture of ethanol and diethylether (40 ml) to precipitate the product. The solid was filtered off, washed with ethanol/diethylether (1:1) and dried in vacuum to yield the bromoacetylated polylysine (**5**) (40 mg, 97%).

^1H NMR (DMSO-d_6): δ = 1.15-1.80 (m, 6H, CH-C$\underline{H}_2$-C$\underline{H}_2$-C$\underline{H}_2$-CH_2), 3.04 (m, 2H, C$\underline{H}_2$-NH), 3.84 (s, 2H, C$\underline{H}_2$-Br), 4.25 (m, 1H, C$\underline{H}$), 7.76 (m, 2H, NH).

*Preparation of **6** by coupling of the BFCA to the* bromoacetylated polylysine *(**5**). p-*NH_2-Bn-DTPA•4 HCl (48 mg, $74.5*10^{-3}$ mmol) was dissolved in dry DMSO (2 ml) and cooled to 0°C. DIPEA (0.08 ml, 0.46 mmol) was added slowly and the reaction solution was stirred for 20 min. Then, bromoacetylated polylysine (**5**) (11 mg) and NaI (9 mg, 0.06 mmol) were dissolved in DMSO (0.5 ml) and added dropwise over 30 min. to the reaction mixture, which was allowed to stir for 20 h at 0°C. The solution

was added dropwise to a 1:1 mixture of ethanol and ether (40 ml) to precipitate the product. The solid was filtered off, washed with ethanol/ether (1:1) and dried to yield the desired product **6** (19 mg, 65%).

^{1}H NMR (DMSO-d_6): δ = 0.86 (m, 2H, CH-CH_2-C$\underline{H}_2$), 1.06 (m, 2H, C$\underline{H}_2$-CH_2-NH), 1.24 (m, 2H, CH-C$\underline{H}_2$-CH_2), 1.99 (m, 1H, NH), 2.10-2.85 (m, 8H, N-C$\underline{H}_2$-C$\underline{H}_2$-N; N-CH-C$\underline{H}_2$-N; Ar-C$\underline{H}_2$), 2.90-3.89 (m, 14H, C$\underline{H}_2$-NH-CO; C$\underline{H}_2$-COOH; NH-C$\underline{H}$-CO), 6.49 (m, 2H, Ar-$\underline{H}$), 6,82 (Ar-$\underline{H}$).

Results and Discussion

The development of an active ester mediated attachment of a bifunctional chelating agent to lysine residues of peptides or carrier proteins for the purpose of MRI diagnosis and potential drug delivery started with the choice of a suitable test system. Economical reasons due to expensive reagents and easy handling and characterization of the employed replacement substances facilitated development activities.

Fmoc protected lysine was favored due to good characterization conditions. Modifications at any position can easily be identified by nuclear magnetic resonance (NMR) and electrospray ionization mass spectrometry (ESI-MS). Separation from excess reagent without significant loss of product is straight forward using column chromatography.

In comparison to the bifunctional chelating agent *p*-NH_2-Bn-DTPA - containing five carboxylic acid functionalities and several methylene positions - the replacement

compound para-aminobenzoic acid consists of aniline and just one carboxylic acid functionality. The simple structure is easily characterized by NMR. This fact qualified para-aminobenzoic acid as a well applicable substitution for the BFCA.

Since active esters of bromoacetic acid like 4-nitrophenyl or N-succinimidyl esters provide low selectivity for acylation in the presence of primary amine groups a significant amount of n-alkylated side products will be formed. In contrast, the employment of stable bromoacetic acid esters of electron deficient phenols as activation reagent showed the predominant formation of the desired bromoacetylation product and marginal n-alkylation side reactions (*20*). Beyond that, fluorophenyl esters display better stability towards hydrolysis in basic aqueous solutions than the corresponding N-hydroxysuccinimide ester. The esterification proceeded by the employment of DCC to activate the carboxylic functionality. The product (**1**) was obtained in 83% yield after purification by Kugelrohr distillation.

Bromoacetylation of Fmoc lysine succeeded under amide formation at the terminal *ε*-amine of the amino acid with active ester (**1**). After isolation of the product (**2**) the NMR spectrum indicated that no undesired n-alkylation - side reaction occurred. Purified **2** was obtained in 61% yield (Figure 1).

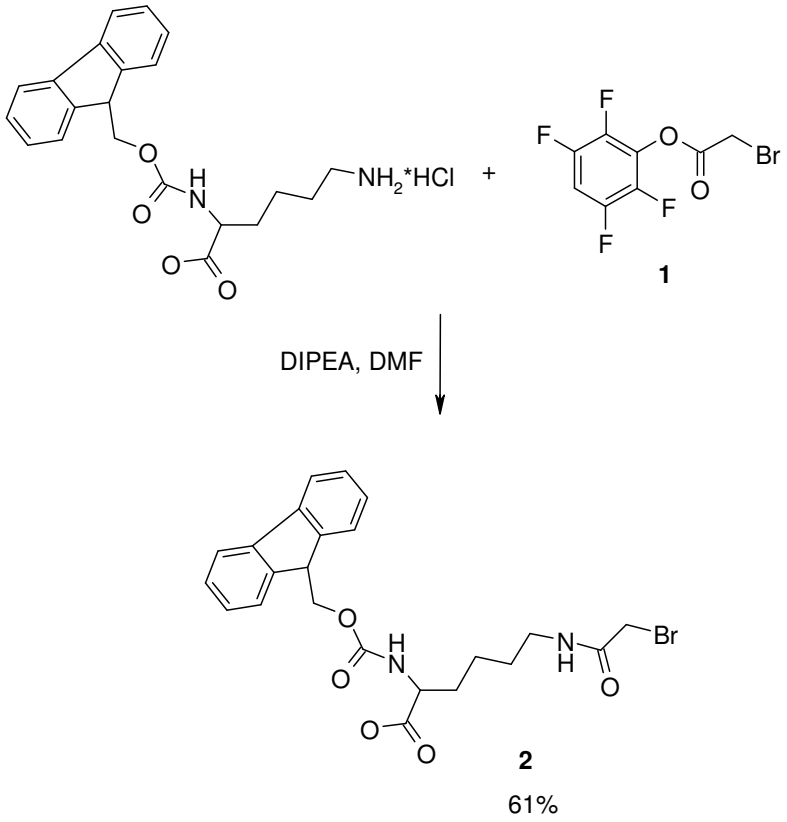

Figure 1. Bromoacetylation of Fmoc lysine.

The following n-alkylation of the primary amine of *p*-aminobenzoic acid and the bromoacetate (**2**) was performed under alkaline conditions to give **3** in 88% yield, after purification by column chromatography (Figure 2).

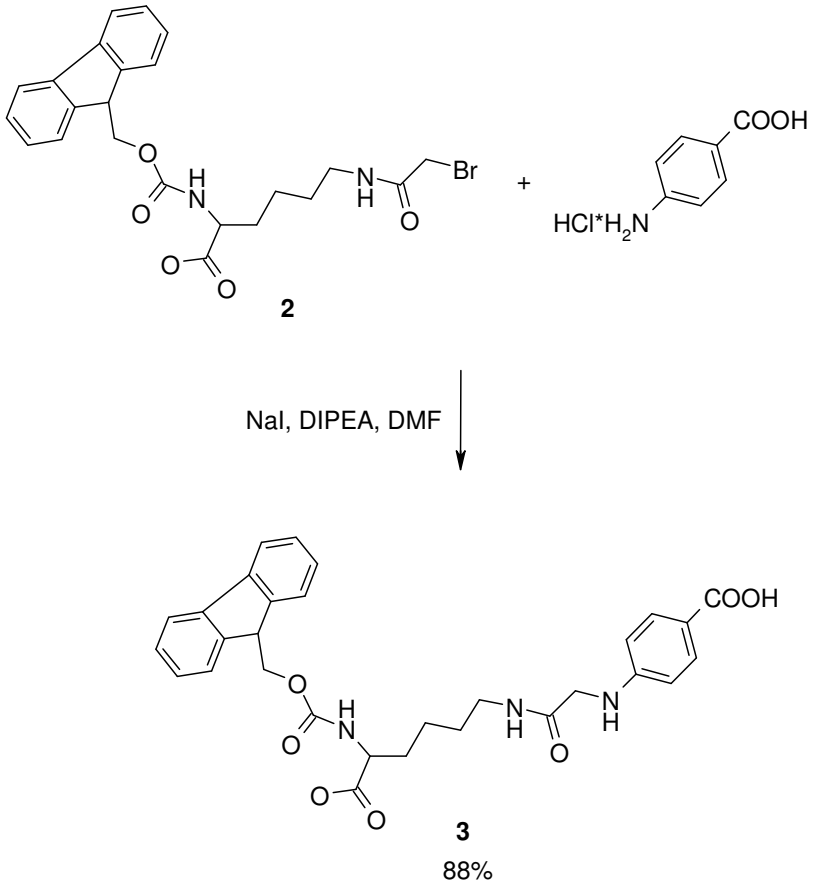

Figure 2. N-alkylation of para-aminobenzoicacid with **2**.

Following this successful n-alkylation, the same conditions were applied to the conversion of the bromoacetylated Fmoc lysine and *p*-NH_2-Bn-DTPA into the bifunctional ligand. Unfortunately, the resulting product was difficult to isolate from unconverted material by column chromatography. Nevertheless, ESI-MS data indicated the presence of **4** (Figure 3).

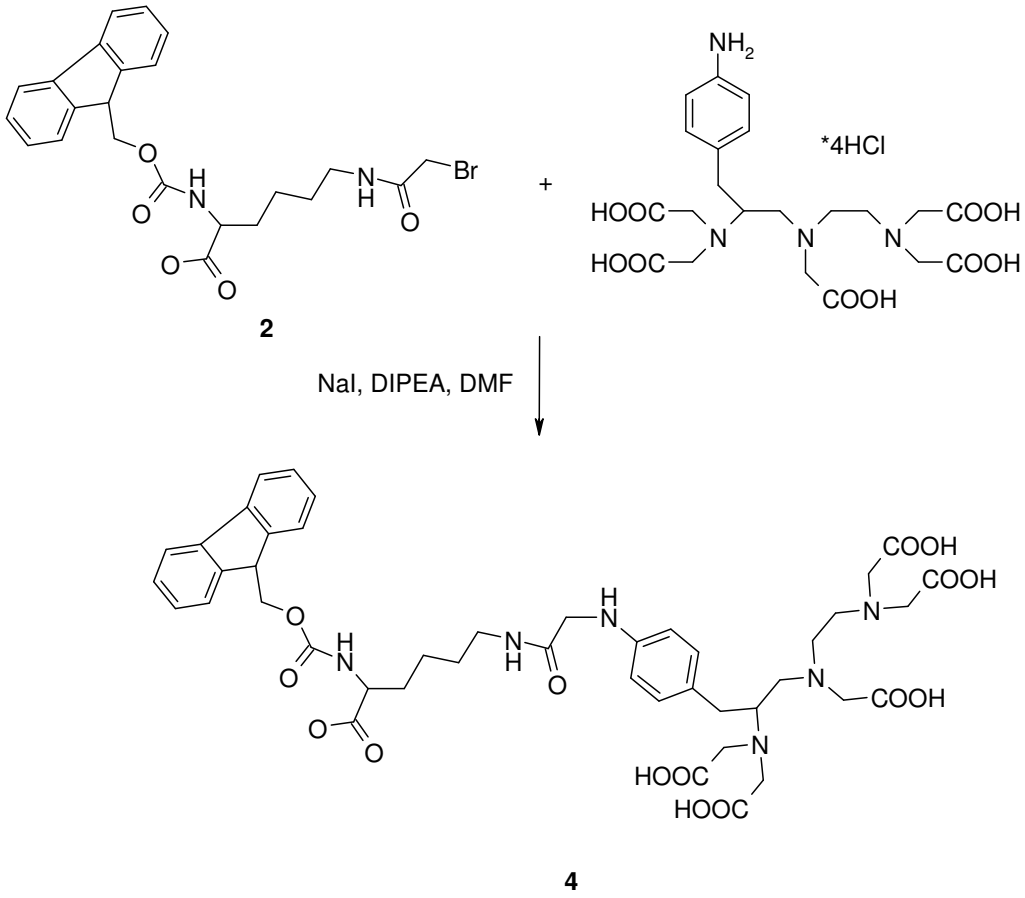

Figure 3. N-alkylation of p-NH_2-Bn-DTPA with **2**.

Polylysine of different molecular weight fractions are well characterized and commercially available. This polyamino acid is non-immunogenic and biodegradable. Acylated polylysine derivatives have already been explored as drug carrier (*21*,*22*). The bromoacetylation of polylysine was carried out by the adaptation of a literature procedure (*23*). A cooled suspension of polylysine hydrobromide in a mixture of DMF and 2,6-lutidine was treated with the active ester **1**. Overnight, the suspension formed a clear solution. This indicated the conversion of the reagents. The bromoacetylated product **5** was isolated by precipitation from a 1:1 mixture of ethanol and diethylether. The yield was calculated by the ratio of the molecular weight of polylysine

hydrobromide (mw: 15000-3000) and the molecular weight of the derivatized product **5** (mw: 17676-35601). The molecular weight ratio is 1.17. Multiplication of the amount of the starting material with 1.17 results in the substance weight for 100% conversion. Applying this calculation the reaction gave 97% yield. The product **5** is insoluble in water but readily soluble in DMSO.

Again, n-alkylation with *p*-NH_2-Bn-DTPA was performed under basic conditions and the resulting compound was isolated by precipitation from an EtOH/Et_2O (1:1) mixture. After drying 65% of the product **6** were obtained (Figure 4).

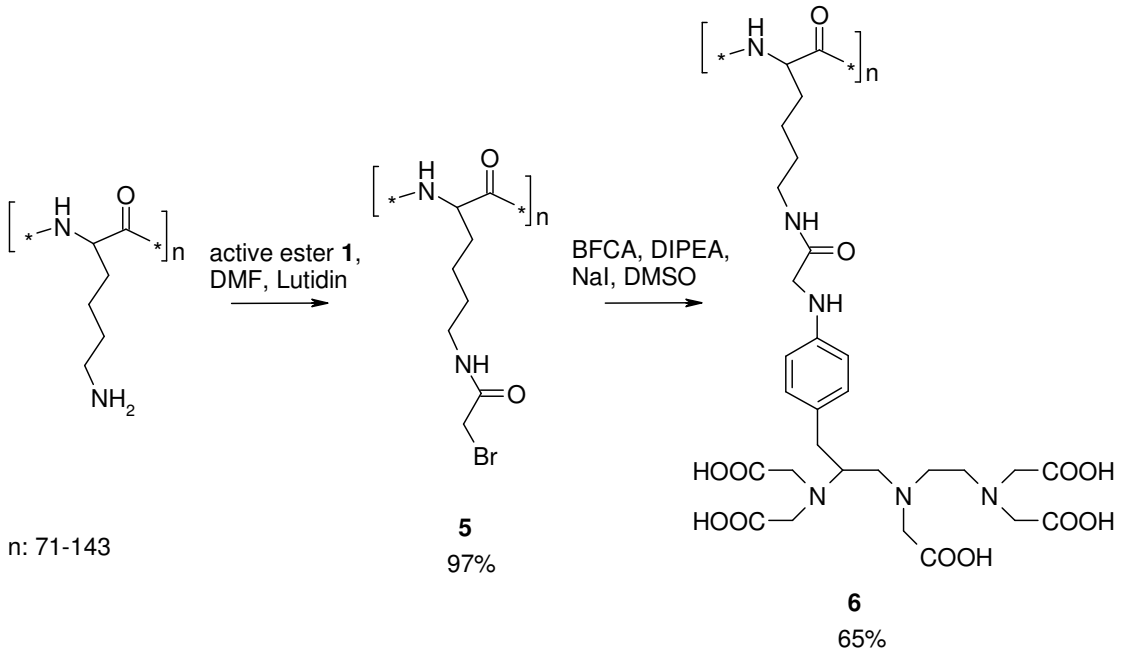

Figure 4. Bromoacetylation of polyylsine and subsequent n-alkylation.

In conclusion a novel strategy for the functionalization and covalent conjugation of a bifunctional chelating agent to the terminal *ε*-amines of lysine moieties was

presented. The bromoacetylation of Fmoc protected lysine and polylysine were performed with a novel active ester in good yields. Subsequent n-alkylation with the primary amine functionality of the DTPA derivative resulted in the desired products. This novel active ester mediated conjugation can be applied to similar systems containing biomacromolecules with lysine residues and primary amine groups of low molecular weight ligands.

References

1) Merbach, A. E., Tóth, É. (2001) The Chemistry of Contrast Agents in Medical Magnetic Resonance Imaging. John Wiley & Sons, New York

2) Caravan, P., Ellison, J. J., McMurry, T. J., Lauffer, R. B. (1999) Gadolinium (III) Chelates as MRI Contrast Agents: Structure, Dynamics, and Applications. *Chem. Rev. 99*, 2293-2352

3) Sieber, M.A., Pietsch, H., Walter, J., Haider, W., Frenzel, T:, Weinmann, H. J. (2008) A Preclinical Study to Investigate the Development of Nephrogenic Systemic Fibrosis: A Possible Role for Gadolinium-Based Contrast Media. *Invest. Radiol. 43*, 65-75.

4) Hermann, P., Kotek, J., Kubíček, V., Lukeš, I. (2008) Gadolinium (III) complexes as MRI contrast agents: ligand design and properties of the complexes. *Dalton Trans*. 3027-3047.

5) Barrett, T., Kobayashi, H., Brechbiel, M., Choyke, P. L. (2006) Macromolecular MRI contrast agents for imaging of tumor angiogenesis. *Eur. J. Radiol. 60,* 353-356.

6) Brasch, R. C., Daldrup-Link, H. E. (2003) Macromolecular contrast agents for MR mammography: current status. *Eur. Radiol. 13*, 354-365.

7) Sirlin, C. B., Vera, D. R., Corbeil, J. A., Caballero, M. B., Buxton, R. B., Mattrey, R. F. (2004) Gadolinium-DTPA-dextran: a macromolecular MR blood pool contrast agent. *Acad. Radiol. 11*, 1361-1369.

8) Xu, H., Regino, C. A. S., Koyama, Y., Hama, Y., Gunn, A. J., Bernardo, M., Kobayashi, H., Choyke, P. L., Brechbiel, M. W. (2007) Preparation and preliminary evaluation of a biotin-targeted, lectin-targeted dendrimer-based probe for dual modality magnetic resonance and fluorescence imaging. *Bioconjugate Chem*. *18*, 1474–1482.

9) Kido, N., Xu, H., Regino, C. A. S., Bernardo, M., Ileva, L., Riffle, L., Wong, K. J., Brechbiel, M. W. (2009) A New Approach in the Preparation of Dendrimer-Based Bifunctional Diethylenetriaminepentaacetic Acid MR Contrast Agent Derivatives. *Bioconjugate Chem. 20*, 1412-1418.

10) Xu, H., Regino, C. A. S., Bernardo, M., Koyama, Y., Kobayashi, H., Choyke, P. L., Brechbiel, M. W. (2007) Towards Improved Syntheses of Dendrimer-Based Magnetic Resonance Imaging Contrast Agents: New Bifunctional Diethylenetriaminepentaacetic Acid Ligands and Nonaqueous Conjugation Chemistry. *J. Med. Chem. 50*, 3185-3193.

11) Langereis, S., de Lussanet, Q. G., van Genderen, M. H., Meijer, E. W., Beets-Tan, R. G., Griffioen, A. W., van Engelshoven, J. M., Backes, W. H. (2006) Evaluation of Gd (III) DTPA-terminated poly(propylene imine) dendrimers as contrast agents for MR imaging. *NMR Biomed. 19*, 133-141.

12) Ogan, M. D., Schmiedl, U., Moseley, M. E., Grodd, W., Paanjanen, H., Brasch, R. C. (1987) Albumin labeled with Gd-DTPA. An intravascular contrast enhancing agent for magnetic resonance blood pool imaging: preparation and characterization. *Invest. Radiol. 22*, 665-671.

13) Schuhmann-Giampieri, G., Schmitt-Willich, H., Frenzel, T., Press, W. R., Weinmann, H. J. (1991) In Vivo and In Vitro Evaluation of Gd-DTPA-Polylysine as a Macromolecular Contrast Agent for Magnetic Resonance Imaging. *Invest. Radiol. 26*, 969-974.

14) Spanoghe, M., Lanens, D., Dommisse, R., Van der Linden, A., Alderweireldt, F. (1992) Proton relaxation enhancement by means of serum albumin and poly-L-lysine labelled with DTPA-Gd^{3+}: relaxivities as a function of molecular weight and conjugation efficiency. *Magnetic Resonance Imaging 10*, 913-917.

15) Bogdanov, A. A., Lewin, M., Weissleder, R. (1999) Approaches and agents for imaging the vasculature system. *Adv. Drug Del. Rev. 37*, 279-293.

16) Fu, Y., Raatschen, H. J., Nitecki, D. E., Wendland, M. F., Novikov, V., Fournier, L. S., Cyran, C., Rogut, V., Shames, D. M., Brasch, C. R. (2007) Cascade Polymeric MRI Contrast Media Derived from Poly(ethylene glycol) Cores: Initial Syntheses and Characterizations. *Biomacromolecules 8*, 1519-1529.

17) Gugliotta, G., Botta, M., Giovenzana, G. B., Tei, L. (2009) Fast and easy access to efficient bifunctional chelators for MRI applications. *Bioorg. Med. Chem. Lett. 19*, 3442–3444

18) Chong, H. S., Ma, X., Le, T., Kwamena, B., Milenic, D. E., Brady, E. D., Song, H. A., Brechbiel, M. W. (2008) Rational Design and Generation of a Bimodal Bifunctional Ligand for Antibody-Targeted Radiaton Cancer Therapy. *J. Med. Chem. 51,* 118-125.

19) Cummins, C. H., Rutter, E. W., Fordyce, W. A. (1991) A Convenient Synthesis of Bifunctional Chelating Agents Based on Diethylenetriaminepentaacetic Acid and their Coordination Chemistry with Yttrium(III). *Bioconjugate Chem. 2*, 180-186.

20) Heine, N., Ast, T., Schneider-Mergener, J., Reineke, U., Germeroth, L., Wenschuh, H. (2003) Synthesis and screening of peptoid arrays on cellulose membranes. *Tetrahedron 59*, 9919-9930.

21) Nègre, E., Monsigny, M., Mayer, R. (1993) Synthesis of an allopurinol riboside-mannosylated poly-L-lysine conjugate. *Tetrahedron 49,* 6991-7000.

22) Gonsho, A., Irie, K., Susaki, H., Iwasawa, H. (1994) Tissue-targeting ability of saccharide-poly(L-lysine) conjugates. *Biol. Pharm. Bull. 17,* 275-282.

23) Thoma, G., Patton, J. T., Magnani, J. L., Ernst, B., Öhrlein, R., Duthaler, R. O. (1999) Versatile Functionalization of Polylysine: Synthesis, Characterization, and Use of Neoglycoconjugates. *J. Am. Chem. Soc. 121,* 5919-5929.

Strategies for the covalent conjugation of a bifunctional chelating agent to albumin: synthesis and characterization of potential MRI contrast agents

Amitava Kundu[†], Herwig Peterlik[‡], Martin Krssak[§], Anna K. Bytzek[†], Thomas H. Helbich[§], Bernhard K. Keppler[†,*]

[†] Institute of Inorganic Chemistry, University of Vienna; [‡] Faculty of Physics, University of Vienna; [§] Department of Radiology, Medical University of Vienna; [*] Correspondence to Bernhard K. Keppler, Institute of Inorganic Chemistry, Waehringer Strasse 42, A-1090 Vienna, Tel: +43 1 4277 52602, Fax: +43 1 4277 52680, E-mail: bernhard.keppler@univie.ac.at

Running title: Albumin Based Potential MRI Contrast Agents

Abstract

With the purpose to develop macromolecular magnetic resonance imaging contrast agents, we herein report three different synthetic approaches to the covalent attachment of bifunctional chelating agents to human serum albumin followed by coordination to contrast enhancing Gd(III). Applied methods cover active ester-mediated conjugation, linkage through glutaryl spacer, as well as the connection by the employment of glutaraldehyde. The content of Gd(III) was evaluated by ICP-MS measurements and indicated reproducible amounts of conjugated contrast enhancing material. Small angle X-ray scattering experiments provided the size dimension and altered shape of the gadolinium loaded proteins in comparison to unmodified albumin. Finally, the relaxation behavior of the protein conjugates was evaluated and indicated suitability for the use as macromolecular contrast agent.

Introduction

The use of metals as diagnostic agents has become a powerful tool in medicine. Especially magnetic resonance imaging (MRI) provides a noninvasive and high spatial resolution imaging technique (*1,2*). At present, the most widespread applied paramagnetic contrast enhancing metal is the lanthanide gadolinium. Free Gd(III) however, is toxic and may harm spleen, liver, bones and can also cause nephrogenic systemic fibrosis (NSF) (*3*). Therefore, stable polyaminocarboxylic acid derived gadolinium chelates are commonly employed.

Gadolinium chelating ligands of clinically approved contrast agents (CA) are throughout based on the structural backbone of the linear diethylenetriaminepentaacetic acid (DTPA) or the macrocyclic 1,4,7,10-tetraazacyclododecane-*N,N',N'',N'''*-tetraacetic acid (DOTA). Paramagnetic gadolinium compounds with multidentate ligands like Gd-DTPA (Magnevist®), Gd-DTPA-BMA (Omniscan®), Gd-DTPA-BMEA (OptiMARK®), Gd-BOPTA (MultiHance®), Gd-EOB-DTPA (Primovist®) and the cyclic Gd-DOTA (Dotarem®), Gd-HP-DO3A (ProHance®) and Gd BT-DO3A (Gadovist®) are currently in use (*4*). Though, these low molecular weight agents suffer from the disadvantage of diffusion from the vasculature into the interstitial space and rapid renal excretion (*5*).

Contrast media in which numerous Gd(III) ions are covalently attached to a nanosphere have shown promise to overcome the limitations of low molecular weight agents. It is supposed that macromolecular contrast media define a blood-tissue barrier comparable to the existing barrier for large molecular endogenous substances in the blood like plasma proteins and hematopoietic cells (*6*). These so called Blood Pool Agents have been designed for prolonged intravascular retention

and hence, to increase molar relaxivities from the vasculature over an extended period of time.

Among a variety of nanosized carriers used for the attachment to gadolinium chelates, dextran is investigated due to its well established safety profile and biocompatibility. It can be synthesized to integrate a high density of gadolinium without intra-molecular cross-linking (*7*). Furthermore, it has a large number of hydroxyl groups suitable for additional conjugation to drugs. Nanoparticles consisting of a polysaccharide backbone covalently derivatized with gadolinium complexing chelating ligands have also been studied and indicated enhanced T1 relaxivity (*8*). Another type of macromolecular carrier are liposomes. They can be formed in different diameters varying from 20 to 400 nm with incorporated contrast enhancing substances. A rigorous drawback in the development of liposomes as nanosized contrast media is their polydispersity which hinders a reproducible synthesis (*5*). The syntheses of polyethylene glycol attached lysine cascades nanospheres have also been reported and indicated strong, prolonged MRI enhancement of vessels (*9*). Much attention has been paid to the possible application of dendrimers as nanospheres for macromolecular contrast agents (*5,10,11,12,13*). Dendrimers are highly branched synthetic polymers with a well defined structure and can be produced reproducibly with specific sizes. Gadolinium loaded albumin as macromolecular contrast agents has been investigated since 1987 when Gd-DTPA was covalently linked via amide formation to albumin molecules (*14*). The convenience of using serum proteins is based on their biocompatibility, stability and extended intravascular retention. Conjugations of Gd-DTPA or Gd-DOTA derivatives to albumin show high relaxivities and moreover, they are comparatively cheap and can easily be obtained (*5,15*). A non covalent attachment of a DTPA derivative to

human serum albumin is the strategy of the chelator MS 325 (*16,17*). This albumin targeted agent is specifically designed for blood vessel imaging. It is clinically approved and commercially available under the trademark Vasovist®. In this molecule, the DTPA backbone was modified by a phosphodiester linked biphenylcyclohexyl moiety. MS 325 binds reversibly to human serum albumin in plasma.

To avoid possible weakening of the gadolinium complexation that may lead to the release of free Gd(III) ions a number of bifunctional chelating agents (BFCA) have been developed (*12,18,19*). Bifunctional ligands have been designed to bind tightly to the metal ion while a further functionality acts as a linker to the macromolecule.

In this study, we introduce three strategies for the covalent conjugation of a bifunctional chelating agent to human serum albumin and the complexation to Gd(III). The first method describes the activation of human serum albumin (HSA) through bromoacetic acid, 2,3,5,6-tetrafluorophenyl ester and subsequent N-alkylation with the primary amine functionality of 2-(*para*-aminobenzyl)-diethylenetriaminepentaacetic acid (NH_2-Bn-DTPA). The further techniques enable covalent attachment by the application of glutaric acid anhydride and glutaraldehyde. The following complexation of the albumin bound DTPA derivative with Gd(III) and the evaluation of the amount of chelated metal are reported as well. Additionally, we report the structure and size dimension of the Gd(III) labeled albumins shown by small angle X-ray scattering (SAXS) measurements. Finally, the effects on the relaxation behavior were investigated and will be presented in this paper.

Experimental Procedures

Materials and Methods. Human serum albumin (HSA), phosphate buffered saline (1×PBS), bromoacetic acid, glutaric dialdehyde (50 wt.% solution in water), glutaric anhydride and sodium cyanoborohydride ($NaBH_3CN$) as well as trisodium citrate dihydrate and citric acid monohydrate for buffer preparation were purchased from Sigma-Aldrich (Germany). 2,3,5,6-tetrafluorophenol and dimethylformamide (DMF, extra dry) were obtained from Acros (Belgium). *N*-(3-dimethylaminopropyl)-*N´*-ethyl-carbodiimide hydrochloride (EDC), *N,N´*-dicyclohexylcarbodiimide (DCC) and sodium bicarbonate were purchased from Fluka (Germany). Trisodium bis(nitrilotriacetate)gadolinate solution ($Na_3[Gd(NTA)_2]$) (*20*) as well as 2-(*para*-aminobenzyl)-diethylenetriaminepentaacetic acid tetrahydrochloride (NH_2-Bn-DTPA·4 HCl) (*21*) were prepared according to literature procedures. All water used was purified by a Millipore Synergy 185 UV Ultrapure Water System (Molsheim, France). NMR spectra were recorded at 24 °C on a Bruker Avance DPX400 spectrometer (Ultrashield magnet) at 400.13 MHz (^1H) and 100.63 MHz (^{13}C). Elemental analyses were carried out with a Perkin-Elmer 2400 CHN elemental analyzer or by titration with an automatic titration system using 0.1 M $AgNO_3$ (DL 21, Mettler-Toledo, 1990) after Schöniger-decomposition (for Br), respectively at the Microanalytical Laboratory of the University of Vienna.

Preparation of **3** by active ester mediated conjugation of NH_2-Bn-DTPA to HSA.

Bromoacetic acid, 2,3,5,6-tetrafluorophenylester (**1**). Bromoacetic acid (1.13 g, 8.15 mmol) and 2,3,5,6-tetrafluorophenol (1.36 g, 8.20 mmol) were dissolved in CH_2Cl_2 (30 ml) and cooled to 0°C. A small amount of molecular sieve (3 Å) was added. DCC

(1.88 g, 9.13 mmol) was dissolved in dichloromethane (15 ml) and added slowly to the reaction solution. After 45 min. the cooling bath was removed and the reaction was allowed to stir for further 45 min. at ambient temperature. Thereafter, the organic layer was extracted four times with water, dried over anhydrous Na_2SO_4 and evaporated under reduced pressure. Finally, the product was purified by Kugelrohr distillation (1.2×10^{-1} mbar, 63°C) to yield the product as colorless oil (1.95 g, 6.80 mmol, 83%). ^{1}H NMR ($CDCl_3$):δ= 4.14 (s, 2H), 7.04 (m, 1H); ^{13}C NMR ($CDCl_3$): δ= 23.7 (CH_2), 104.1 (CH, Ar), 129.3 (C, Ar), 139.6 – 141.7 (CF, Ar), 145.2 – 147.3 (CF, Ar), 163.6 (CO); Elemental analyses: calcd for $C_8H_3BrF_4O_2$: C, 33.48; H, 1.05; Br, 27.84. Found: C, 33.50; H, 0.95; Br, 28.39.

Activation of HSA: HSA (53.6 mg, 0.8×10^{-3} mmol) was dissolved in PBS (12 ml). Bromoacetic acid, 2,3,5,6-tetrafluorophenylester (**1**) (43 mg, 149.8×10^{-3} mmol) dissolved in DMF (1.7 ml) was added slowly to the albumin solution and the pH was maintained within a range of 7.8 – 8 by the addition of 0.1 M NaOH. Next, the reaction mixture was stirred for 2 h at room temperature. To remove excess reagents and small molecular compounds the solution was concentrated by centrifugation (Vivaspin 20, MWCO: 30000, 2500×g, 19°C) and repeatedly washed with water (three times).

*N-alkylation of NH_2-Bn-DTPA (**2**)*: The activated HSA was dissolved in 0.1 M $NaHCO_3$ (pH 8.1) (10 ml) and NH_2-Bn-DTPA·4HCl (46.8 mg, 72.6×10^{-3} mmol) in 0.1 M $NaHCO_3$ (2 ml) was added slowly to this solution while maintaining the pH between 8 and 8.5 by the addition of 0.3 M NaOH. Afterwards, the reaction mixture was stirred for 18 h at room temperature. Finally, the solution was concentrated again by centrifugation (Vivaspin 20, MWCO: 30000, 2500×g, 19°C) and repeatedly washed with water (three times).

Complexation to Gd(III): Albumin conjugated NH_2-Bn-DTPA was dissolved in 7 ml 0.1 M citric buffer (pH 6.5) and cooled to 4°C. 0.1 M $Gd(NTA)_2$ solution (2.5 ml, 0.25 mmol) was added and allowed to react for 21 h. The solution was concentrated by centrifugation (Vivaspin 20, MWCO: 30000, 2500×g, 19°C) and washed with water (three times) yielding an aqueous solution of **3**.

Preparation of **4** by glutaric anhydride mediated conjugation of NH_2-Bn-DTPA to HSA.

Glutarylation of HSA: HSA (53 mg, 0.8×10^{-3} mmol) was dissolved in 0.1 M $NaHCO_3$ (10 ml) and cooled to 4°C. Glutaric anhydride (62 mg, 543.4×10^{-3} mmol) was added slowly in small portions. Repeatedly, the pH of the mixture was adjusted within a range of 7.8 - 8.2 by addition of 0.6 M NaOH. Then the solution was stirred for 22 h at 4°C. Afterwards, the solution was concentrated by centrifugation (Vivaspin 20, MWCO: 30000, 2500×g, 19°C) and repeatedly washed with water (three times).

*Linkage to NH_2-Bn-DTPA (**2**)*: The glutarylated albumin was diluted with H_2O (7 ml) and NH_2-Bn-DTPA·4HCl (60 mg, 931×10^{-3} mmol) in H_2O (2 ml) was added at room temperature. During the addition, the pH was kept at 6.8 - 7.2 by addition of 0.3 M NaOH. EDC (8 mg) was added to the solution and the conjugation reaction proceeded for 2 h at room temperature. For the removal of excess reagents and low molecular weight compounds, the solution was concentrated by centrifugation (Vivaspin 20, MWCO: 30000, 2500×g, 19°C) and repeatedly washed with water (three times).

Complexation to Gd(III): Albumin conjugated NH_2-Bn-DTPA was then dissolved in 0.1 M citric buffer (10 ml) (pH 6.5) and cooled to 4°C. 0.1 M $Gd(NTA)_2$ solution (2.5 ml, 0.25 mmol) was added and allowed to react for 19 h. Finally, the reaction mixture was concentrated by centrifugation (Vivaspin 20, MWCO: 30000, 2500×g, 19°C) and repeatedly washed with water (three times) to give a purified aqueous solution of **4**.

Preparation of **5** by glutaric dialdehyde mediated conjugation of NH_2-Bn-DTPA to HSA.

Conjugation and complexation with Gd(III): HSA (49 mg, 0.7×10^{-3} mmol) and NH_2-Bn-DTPA·4HCl (38.7 mg, 60.1×10^{-3} mmol) were dissolved in PBS (15 ml) and cooled to 4°C. The pH was adjusted with 3 M NaOH to 8.0. Glutaric dialdehyde (1 ml, 5.52 mmol) was dropped slowly to the reaction mixture and the pH was maintained at 7.6 - 8.1 by the addition of 0.1 M NaOH. Then, the mixture was stirred for 2 h at 4°C. 2 M $NaBH_3CN$ (solution in 0.01 M NaOH) (0.89 ml, 1.782 mmol) was added slowly and the pH was adjusted repeatedly to 8.0 with 1 M HCl. Again, the solution was stirred for 1 h at 4°C. Finally, the pH was altered to 6.7 by 1 M HCl and 0.1 M $Gd(NTA)_2$ solution (2 ml, 0.2 mmol) was added at 4°C and allowed to react for 19 h. The reaction mixture was concentrated and washed with water (three times) by centrifugation (Vivaspin 20, MWCO: 30000, 2500×g, 19°C) to yield an aqueous solution of **5**.

Characterization.

Protein Assay. The protein concentration of purified gadolinium loaded albumin solutions was determined by the method of Bradford. A Bradford test kit from Bio-Rad Laboratories (Vienna, Austria) was used and adapted for usage in 96 - well plates. Optical densities at 595 nm were recorded on a microplate reader (Synergy HT, Biotek) 15 min. after the addition of the Bradford solution.

Inductively Coupled Plasma Mass Spectrometry (ICP-MS). The gadolinium content of the purified albumin solutions was determined by ICP-MS (Agilent 7500ce, Waldbronn, Germany), equipped with a CETAC ASX-520 autosampler (Neuss, Germany), a Scott double pass spray chamber, and a MicroMist nebulizer. For the analysis, the samples were diluted 1:60 000 with 3.5% HNO_3 (HNO_3 p.a. from Sigma Aldrich, further purified with a quartz sub-boiling system from Milestone-MLS GmbH, Leutkirch, Germany). Every sample contained 0.5 ppb In as internal standard (CPI International, Santa Rosa, CA, USA). The Gd standards were made in the range from 23 to 0.1 ppb with a Gd containing solution purchased from Aldrich chemical company (Milwaukee, USA). The determined LOQ was 0.059 ppb.

Small-Angle X-ray Scattering (SAXS). SAXS experiments were performed using a rotating anode generator, equipped with a pinhole camera and CuKα radiation monochromatized and collimated from crossed Göbel mirrors (Nanostar from Bruker AXS, Karlsruhe). The scattered intensities were collected with an area detector (Vantec 2000, gas detector with microgap technology). All X-ray patterns were radially averaged and corrected for background scattering from the solvent to obtain the scattering intensity I(q), where $q = (4\pi/\lambda)\cdot\sin\theta$ is the scattering vector, 2θ the

angle between the incident and the diffracted beam and λ = 0.1542 nm the X-ray wavelength. The measurements were performed at a sample to detector distance of 1.1 m from which a q-range from 0.1 - 2.8 nm^{-1} was covered.

Spin-Lattice and Spin-Spin Relaxivity measurements. Relaxivity measurements were performed on a 3 Tesla whole-body MRI scanner (TimTrio 3 T, Siemens Medical Solutions, Erlangen, Germany) using a whole body coil for excitation and standard head receiver coil for signal reception. Homogeneity of B_1-field was insured by test measurements before the actual measurements of relaxivity. For each agent four dilutions ranging from 0.018 mM to 0.151 mM in PBS with the volume of 1.5 ml were prepared. All probes were measured in standard PE-tubes with a diameter of 0.8 cm. The tubes were placed in the centre of a plastic box surrounded by water heated to 37°C.

For the determination of spin-lattice relaxation times T_1, spin echo inversion recovery (IR) sequences with inversion times from 0 to 3500 ms (TI = 0, 60, 80, 100, 150, 200, 250, 300, 400, 500, 750, 1000, 1250, 1500, 1750, 2000, 2500, 3500 ms) were used. An adiabatic pulse was applied for B1 insensitive inversion. The other parameters were: TR/TE = 5000/8.1 ms; flip angle 180°; 8 turbo factor 11; FOV read 180 × 180 mm; resolution matrix 192 × 192; bandwidth 260 Hz/pixel; and slice thickness 3 mm. The mean values of the signal intensities, the standard deviations, and pixel counts were determined by drawing regions of interest. The area assessed measured between 0.12 cm^2 and 0.14 cm^2; for each measurement series, the measured area was kept identical by copying and pasting the ROI. For all measurements, the

relaxation rates (R_1) and the relaxivities (r_1) were calculated for each substance. The longitudinal relaxation rate (R_1) was calculated using the equation:

$$SI(TI) = A[1-2\exp(-R_1*TI)+\exp(-R_1*TR)] \quad [1]$$

with SI being the signal intensity as a function of TI, “A” accounting for the thermal equilibrium magnetization M0, and TI being the inversion time in ms.

For the determination of individual spin-spin relaxation times (T_2), spin-echo sequence with multiple echoes (NE= 5) ranging from 13.8 ms to 69 ms was used. Repetition time was set to 2500 ms, FOV 160 × 160 mm, resolution matrix 128 × 128, bandwidth 260 Hz/pixel; and slice thickness 3 mm. The mean values of the signal intensities, the standard deviations, and pixel counts were determined by drawing regions of interest. The area assessed measured between 0.12 cm^2 and 0.14 cm^2; for each measurement series, the measured area was kept identical by copying and pasting the ROI. For all measurements, the relaxation rates (R_2) and the relaxivities (r_2) were calculated for each substance. The transversal relaxation rates (R_2) were calculated as the reciprocal value of the slope of semilogarithmic plot of signal intesities at individual echo times and respective echo times.

The relaxivities (r_1, r_2) were calculated as the slope of linear regression of R_1 and R_2 as a function of contrast agent concentration.

Results and Discussion

Since active esters of bromoacetic acid like 4-nitrophenyl or *N*-succinimidyl esters provide low selectivity for acylation in the presence of primary amine groups, this behavior causes the formation of a significant amount of N-alkylation side products. In contrast, the employment of stable bromoacetic acid esters of electron deficient phenols as activation reagent results predominantly in the formation of the desired bromoacetylation product and little N-alkylation side reactions (*22*). In addition, fluorophenyl esters display better stability towards hydrolysis in basic aqueous solutions than the corresponding *N*-hydroxysuccinimide esters. Furthermore, a property of bromoacetyl functionalities is their capability of thioether formation with cysteine thiols (*23*) which may cause a higher degree of protein conjugation.

The activation of the carrier protein by reaction with **1** proceeded at the *ε* - amine of lysine residues under mild basic conditions. Excessive low molecular weight reagents were removed by centrifugation and followed by subsequent N-alkylation with the BFCA (**2**) at pH 7.8 – 8.2. Concurrently, the bromoacetyl group of the active ester (**1**) could have been converted with cystein thiols and thereafter, the acylation reaction with the primary amine of the DTPA derivative proceeded. Nonconjugated chelating agent was then removed by centrifugation (Figure 1).

To avoid Gd(III) binding to albumin, the contrast enhancing metal was introduced in form of a $Gd(NTA)_2$ solution. Nitrilotriacetic acid is a weak complexant for Gd(III) and prevents nonspecific binding of the chelated metal to proteins (*24*). The gadolinium:albumin ratio was determined by the measurement of protein concentration by the Bradford assay and the detection of the metal content by ICP-

MS. This active ester mediated conjugation showed that on average 13 to 15 Gd(III) were chelated and covalently attached to each HSA molecule.

An alternative conjugation strategy is based on the application of glutaric anhydride as linker between HSA and the Gd(III) chelator. The covalent attachment of BFCA (**2**) to the albumin was performed using a modified method as described in literature (*25*). The glutarylation of the albumin succeeded by the addition of glutaric anhydride in small portions to a cooled solution and repeated correction of the pH to 8. After removal of excess anhydride the free carboxylic functionalities of the glutarylated protein were activated with the water - soluble carbodiimide EDC. This procedure enabled amide formation with the phenylamine residue of the bifunctional DTPA derivative **2**. Subsequently, the reaction mixture was purified and the Gd(III) complexation proceeded overnight. Again the solution was washed and concentrated by centrifugation to yield a solution of **4** (Figure 2). Determination of the gadolinium:albumin ratio indicated that 35 to 37 Gd(III) ions were attached per protein by this technique. It has to be mentioned that in one conjugation experiment only 12 Gd(III) atoms per protein molecule were detected.

In a third attempt to covalently modify HSA with Gd, a glutaraldehyde-mediated approach was chosen. Due to its convenient handling this dialdehyde is the most popular homobifunctional reagent for crosslinking proteins and the conjugation of proteins to other amine containing molecules. In aqueous solutions glutaraldehyde forms α,β - unsaturated polymers which are highly reactive towards primary amines. The polymer size and structure is unknown and may be influenced by the age of the glutaraldehyde solution (*23*). The linkage of HSA and NH_2-Bn-DTPA (**2**) proceeded through the formation of Schiff bases with the ε – amine functionalities of the lysine residues of albumin and the primary amine of the chelating agent under mild alkaline

conditions. However, the generated Schiff bases are not stable in an acidic environment and have therefore been reduced to stable secondary amines. This was carried out by the use of a 2 M sodium cyanoborohydride solution. Finally, the reaction mixture was acidified and addition of $Gd(NTA)_2$ solution yielded **5** (Figure 3). After purification and concentration the protein assay and ICP-MS measurements showed an attachment of 3 to 7 gadolinium chelates at each albumin molecule.

Figure 4 shows the background corrected SAXS data for pure HSA, **3** [with 13 Gd(III) per HSA] **4** [35 Gd(III) per HSA] and **5** [7 Gd(III) per HSA]. All data were normalized to the scattered volume which is different due to variations in the diameter of the capillaries. The scattering intensities were numerically fitted using the programs GNOM (*26*) and DAMMIN (*27*). These programs vary the three-dimensional distribution of small units, visualized by spheres, which represent the electron density of the structure. In a Monte-Carlo simulation the density and arrangement of these units is adjusted in order to recover three-dimensional structures from the experimentally obtained one-dimensional scattering curves. At least five Monte-Carlo runs were performed for each sample and a mean electron density map was constructed using the program DAMAVER (*28*).

Regarding modified albumins a slight increase of the protein sizes is observed related to increasing Gd(III) loading. This is visualized in Figure 5 by the radius of gyration. The numerical fits of the SAXS data result in a heart shaped structure for non modified human serum albumin (Fig. 6a). This corresponds well to literature results (*29*). The scattering contrast arises from the different electron densities of HSA and pure water, which can be interpreted as a two phase system. In the case of the modified albumins **3** and **5,** a three phase system is obtained, which is more difficult to interpret. Nevertheless, as shown in Fig. 6b and 6d with an overlay of HSA

(bright parts) and the modified albumin (dark parts), the shape of the protein seems to change slightly: The higher the Gd(III) content, the more the heart-shaped structure seems to open and the shape tends more to be elongated and stretched. This is possibly an effect of the additional electrical charge introduced by the ligands. In the case of the modified albumin **4**, this can be interpreted again as a two-phase system, with the scattering contrast arising from the large electron difference between the high amount of Gd atoms and the background (pure water and HSA), Fig. 6c. As the orientation of the simulations in Figure 6 (HSA and modified albumin, respectively) is not fixed, there are a number of possible alignments of the protein and the Gd(III) loaded protein with respect to each other. However, as a continuation of the structural changes from Figure 6, it is very probable that the gadolinium complexes are attached predominantly to the external parts of the biomolecule.

The Gd(III) loaded albumins were evaluated at 37°C on their ability to modify the relaxation rate of water. Relaxation rates (R_1, R_2) and respective relaxivities (r_1, r_2) measured in PBS at 3T for agents **3 - 5** are given in Table 1. As displayed in the table compound **4** has the highest relaxivity of the tested compounds per carrier molecule. This corresponds to an r_1 of 9.54 $mM^{-1}*sec^{-1}$ relative to gadolinium concentration. Agent **5** showed lower relaxation than **4** which is due to a low number of gadolinium ions attached per protein. Though, calculation of r_1 of the carrier protein to the relaxivity per Gd(III) results in a similar value (7.91 $mM^{-1}*sec^{-1}$). These results indicate that different linkage by glutaric anhydride or glutaraldehyde does not alter the molar relaxivity compared to each other, but influence the amount of attached Gd(III) significantly. In contrast to **4** and **5** the Gd(III) modified albumin **3** derived by active ester mediation showed just low relaxivity values and does not meet the requirements for the application as a macromolecular MRI contrast agent.

In conclusion we presented the feasibility of three different strategies for the covalent coupling of a bifunctional Gd(III) chelator to albumin. Characterization of size, shape and relaxation behaviour indicated compound **4** as the most promising candidate for further investigations. Ongoing studies on the stability of the Gd(III) complexes and the degradability of the protein conjugates in living organisms will further elucidate the potential application of these compounds as nanosized contrast agents.

Tables and Figures

Table 1. Relaxation behavior of the loaded albumins **3 - 5** in dependence of the carrier concentration (HSA).

compound	$c_{carrier}$ [mM]	R_1 [s^{-1}]	r_1 [s^{-1}*mM^{-1}]	R_2 [s^{-1}]	r_2[s^{-1}*mM^{-1}]
3	0.151	1.057	5.807	3.551	15.046
13 Gd(III)/HSA	0.113	0.655		2.608	
	0.056	0.386		1.796	
	0.026	0.312		1.671	
4	0.151	17.927	114.48	66.590	451.83
12 Gd(III)/HSA	0.113	13.155		39.772	
	0.056	6.808		18.516	
	0.026	3.555		8.480	
5	0.151	3.897	23.714	17.780	111.41
3 Gd(III)/HSA	0.075	2.237		8.937	
	0.037	1.230		4.961	
	0.018	0.732		3.003	

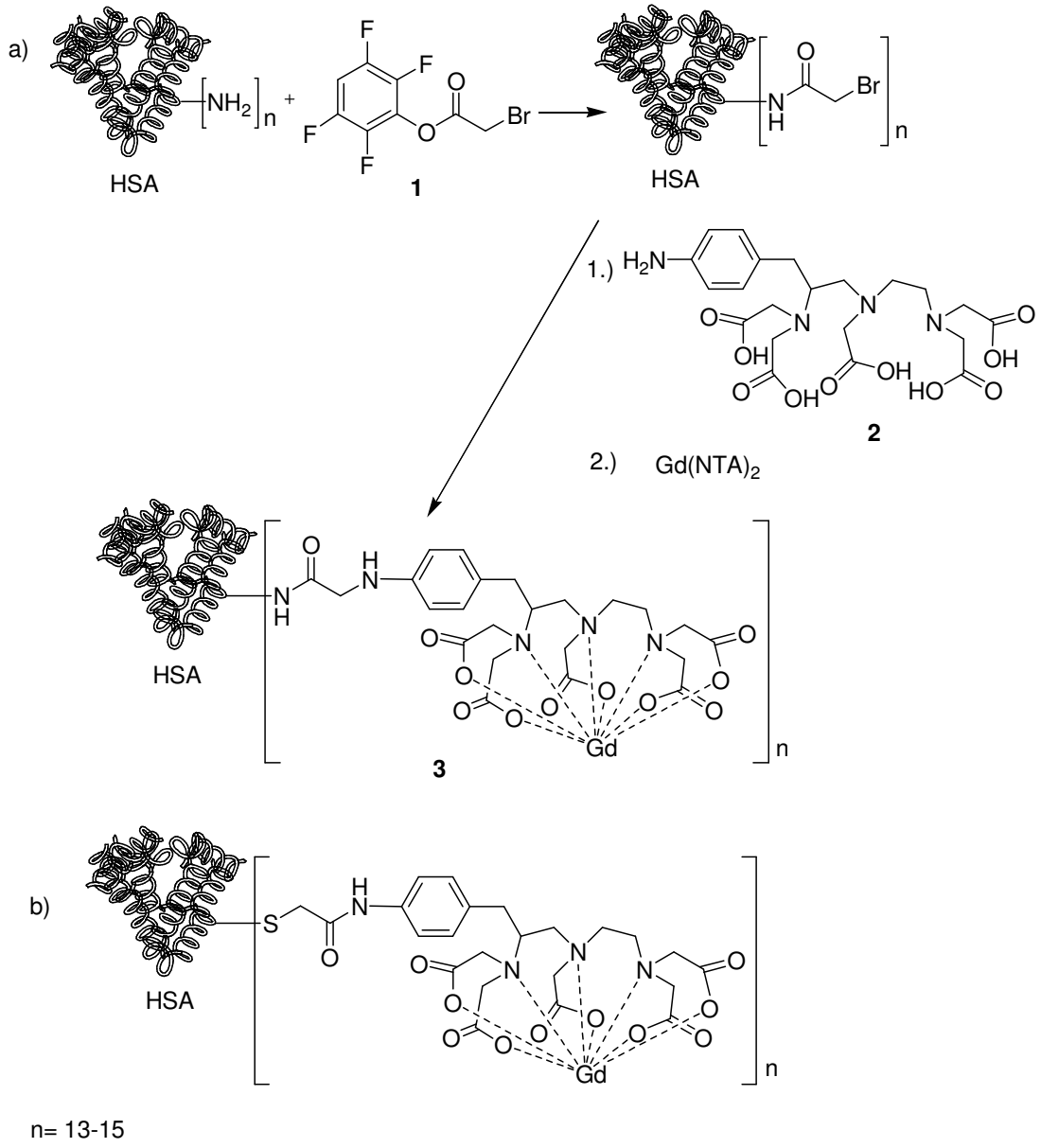

Figure 1. Synthetic scheme of active ester mediated conjugation of Gd(III) chelator **2** at: (a) the *ε* – amines of lysine residues and (b) cysteine thiols.

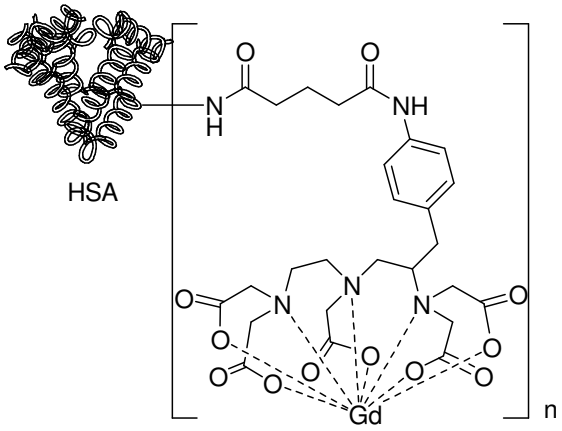

4

n= 35-37

Figure 2. Glutaric anhydride mediated attachment of the BFCA (**2**) to HSA.

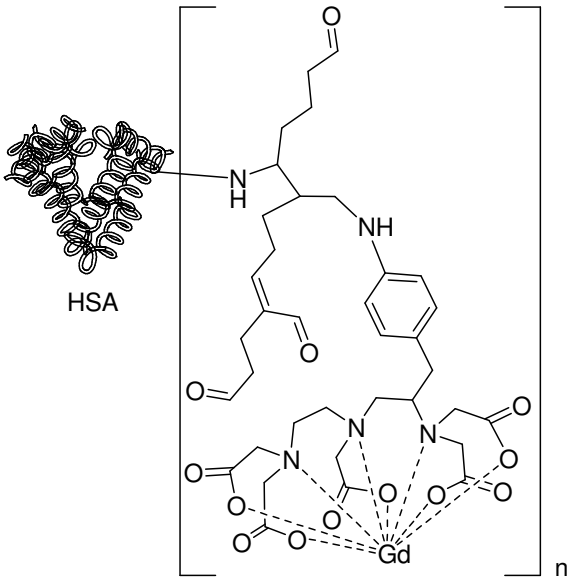

5

n= 3-7

Figure 3. Glutaraldehyde mediated conjugation of **2** to HSA and its Gd(III) complex.

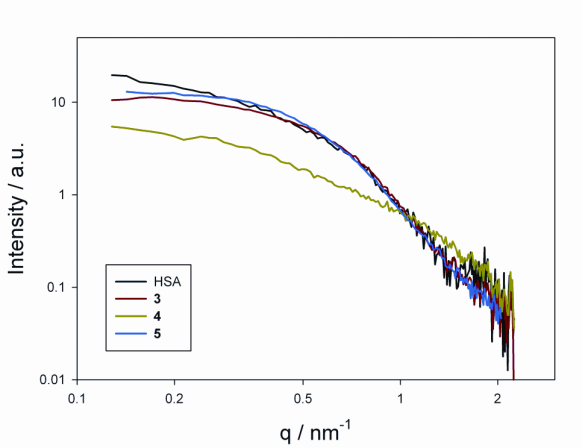

Figure 4. SAXS intensities in dependence on the scattering vector after subtraction of the background.

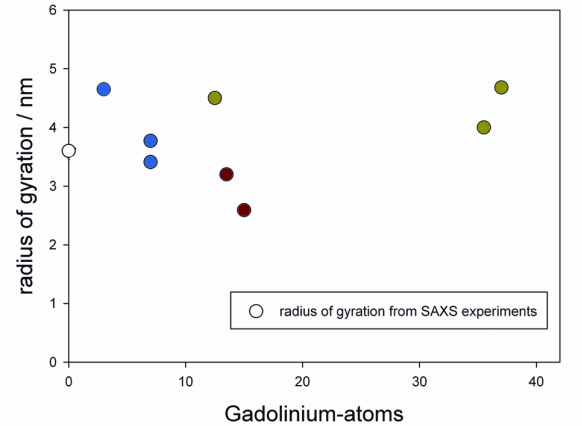

Figure 5. Radius of gyration in dependence of the number of Gd(III): pure HSA (white), **3** (red), **4** (green), **5** (blue).

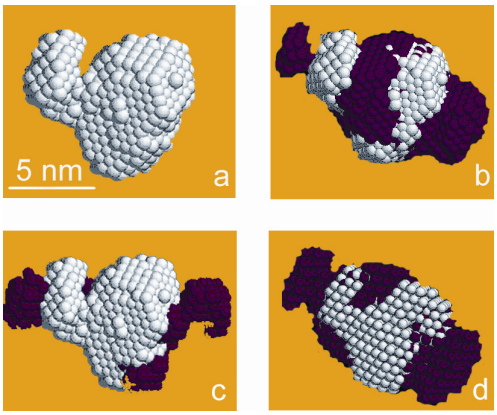

Figure 6. SAXS generated images of pure HSA (a), 13 Gd(III) attached by active ester mediated conjugation (b), 35 Gd(III) attached by glutaric anhydride mediated conjugation (c) and 7 Gd(III) attached by glutaraldehyde mediated conjugation (d).

References

(1) Merbach, A. E., Tóth, É. (2001) The Chemistry of Contrast Agents in Medical Magnetic Resonance Imaging. John Wiley & Sons, New York

(2) Caravan, P., Ellison, J. J., McMurry, T. J., Lauffer, R. B. (1999) Gadolinium (III) Chelates as MRI Contrast Agents: Structure, Dynamics, and Applications. *Chem. Rev. 99*, 2293-2352.

(3) Sieber, M.A., Pietsch, H., Walter, J., Haider, W., Frenzel, T:, Weinmann, H. J. (2008) A Preclinical Study to Investigate the Development of Nephrogenic Systemic Fibrosis: A Possible Role for Gadolinium-Based Contrast Media. *Invest. Radiol. 43*, 65-75.

(4) Hermann, P., Kotek, J., Kubíček, V., Lukeš, I. (2008) Gadolinium (III) complexes as MRI contrast agents: ligand design and properties of the complexes. *Dalton Trans.* 3027-3047.

(5) Barrett, T., Kobayashi, H., Brechbiel, M., Choyke, P. L. (2006) Macromolecular MRI contrast agents for imaging of tumor angiogenesis. *Eur. J. Radiol. 60,* 353-356.

(6) Brasch, R. C., Daldrup-Link, H. E. (2003) Macromolecular contrast agents for MR mammography: current status. *Eur. Radiol. 13*, 354-365.

(7) Sirlin, C. B., Vera, D. R., Corbeil, J. A., Caballero, M. B., Buxton, R. B., Mattrey, R. F. (2004) Gadolinium-DTPA-dextran: a macromolecular MR blood pool contrast agent. *Acad. Radiol. 11*, 1361-1369.

(8) Helbich, T. H., Gossman, A., Mareski, P. A., Radüchel, B., Roberts, T. P. L., Shames, D. M., Mühler, M., Turetschek, K., Brasch, R. C. (2000) A New Polysaccharide Macromolecular Contrast Agent for MR Imaging: Biodistribution and Imaging Characteristics. *J. Magn. Reson. Imaging 11*, 694-701

(9) Fu, Y., Raatschen, H. J., Nitecki, D. E., Wendland, M. F., Novikov, V., Fournier, L. S., Cyran, C., Rogut, V., Shames, D. M., Brasch, C. R. (2007) Cascade Polymeric MRI Contrast Media Derived from Poly(ethylene glycol) Cores: Initial Syntheses and Characterizations. *Biomacromolecules 8*, 1519-1529.

(10) Xu, H., Regino, C. A. S., Koyama, Y., Hama, Y., Gunn, A. J., Bernardo, M., Kobayashi, H., Choyke, P. L., Brechbiel, M. W. (2007) Preparation and preliminary evaluation of a biotin-targeted, lectin-targeted dendrimer-based probe for dual modality magnetic resonance and fluorescence imaging. *Bioconjugate Chem*. *18*, 1474–1482.

(11) Kido, N., Xu, H., Regino, C. A. S., Bernardo, M., Ileva, L., Riffle, L., Wong, K. J., Brechbiel, M. W. (2009) A New Approach in the Preparation of Dendrimer-Based Bifunctional Diethylenetriaminepentaacetic Acid MR Contrast Agent Derivatives. *Bioconjugate Chem. 20*, 1412-1418.

(12) Xu, H., Regino, C. A. S., Bernardo, M., Koyama, Y., Kobayashi, H., Choyke, P. L., Brechbiel, M. W. (2007) Towards Improved Syntheses of Dendrimer-Based Magnetic Resonance Imaging Contrast Agents: New Bifunctional Diethylenetriaminepentaacetic Acid Ligands and Nonaqueous Conjugation Chemistry. *J. Med. Chem. 50*, 3185-3193.

(13) Langereis, S., de Lussanet, Q. G., van Genderen, M. H., Meijer, E. W., Beets-Tan, R. G., Griffioen, A. W., van Engelshoven, J. M., Backes, W. H. (2006) Evaluation of Gd (III) DTPA-terminated poly(propylene imine) dendrimers as contrast agents for MR imaging. *NMR Biomed*. *19*, 133-141.

(14) Ogan, M. D., Schmiedl, U., Moseley, M. E., Grodd, W., Paanjanen, H., Brasch, R. C. (1987) Albumin labeled with Gd-DTPA. An intravascular contrast enhancing agent for magnetic resonance blood pool imaging: preparation and characterization. *Invest. Radiol. 22*, 665-671.

(15) Yan, G. P., Robinson, L., Hogg, P. (2007) Magnetic resonance imaging contrast agents: Overview and perspectives. *Radiography 13*, 5-19.

(16) Caravan, P., Parigi, G., Chasse, J. M., Cloutier, N. J., Ellison J. J., Lauffer, R. B., Luchinat, C., McDermid, S. A., Spiller, M., McMurry, T. J. (2007) Albumin Binding, Relaxivity, and Water Exchange Kinetics of the Diastereoisomers of MS-325, a Gadolinium(III)-Based Magnetic Resonance Angiography Contrast Agent. *Inorg. Chem. 46*, 6632-6639.

(17) Caravan, P. (2009) Protein-Targeted Gadolinium-Based Magnetic Resonance Imaging (MRI) Contrast Agents: Design and Mechanism of Action. *Acc. Chem. Res.42*, 851-862.

(18) Gugliotta, G., Botta, M., Giovenzana, G. B., Tei, L. (2009) Fast and easy access to efficient bifunctional chelators for MRI applications. *Bioorg. Med. Chem. Lett. 19*, 3442–3444.

(19) Chong, H. S., Ma, X., Le, T., Kwamena, B., Milenic, D. E., Brady, E. D., Song, H. A., Brechbiel, M. W. (2008) Rational Design and Generation of a Bimodal Bifunctional Ligand for Antibody-Targeted Radiaton Cancer Therapy. *J. Med. Chem. 51,* 118-125.

(20) Paschkunova-Martic, I., Kremser, C., Mistlberger, K.., Shcherbakova, N.,Dietrich, H., Talaz, H., Zou, Y., Hugl, B., Galanski, M., Sölder, E., Pfaller, K., Höliner, I., Buchberger, W., Keppler, B., Debbage, P. (2005) Design, Synthesis, physical and chemical characterisation, and biological interactions of lectin-targeted latex nanoparticles bearing Gd-DTPA chelates: an exploration of magnetic resonance molecular imaging (MRMI). *Histochem. Cell Biol. 123*, 282-301.

(21) Cummins, C. H., Rutter, E. W., Fordyce, W. A. (1991) A Convenient Synthesis of Bifunctional Chelating Agents Based on Diethylenetriaminepentaacetic Acid and their Coordination Chemistry with Yttrium(III). *Bioconjugate Chem. 2*, 180-186.

(22) Heine, N., Ast, T., Schneider-Mergener, J., Reineke, U., Germeroth, L., Wenschuh, H. (2003) Synthesis and screening of peptoid arrays on cellulose membranes. *Tetrahedron 59*, 9919-9930.

(23) Hermanson, G. T. (2008) Bioconjugate Techniques. 2nd Edition. Elsevier

(24) Spanoghe, M., Lanens, D., Dommisse, R., Van der Linden, A., Alderweireldt, F. (1992) Proton Relaxation Enhancement By Means of Serum Albumin And Poly-L-Lysine Labeled With DTPA-Gd^{3+}: Relaxivities As A Function Of Molecular Weight And Conjugation Efficiency. *MagneticResonance Im*aging *10,* 913-917.

(25) Tanaka, T., Kaneo, Y., Iguchi, S. (1991) Properties of Mitomycin C-Albumin Conjugates in Vitro and in Vivo. *Bioconjugate Chem. 2*, 261-269.

(26) Svergun, D. I. (1992) Determination of the regularization parameter in indirect-transform methods using perceptual criteria. *J. Appl. Cryst. 25*, 495-503.

(27) Svergun, D. I. (1999) Restoring Low Resolution Structure of Biological Macromolecules from Solution Scattering Using Simulated Annealing. *Biophys. J. 76*, 2879-2886.

(28) Volkov, V. V., Svergun, D. I. (2003) Uniqueness of ab initio shape determination in small-angle scattering. *J. Appl. Cryst. 36*, 860-864.

(29) Quinlan, G. J., Martin, G. S., Evan, T. W. (2005) Albumin: Biochemical properties and therapeutic potential. *Hepatology 41*, 1211-1219.

Preparation of gadolinium chelate coated HSA-lectin nanoparticles for magnetic resonance imaging

Amitava Kundu[a], Stephanie Ottofuelling[b], Martin Krssak[c], Frank v.d. Kammer[b], Thilo Hofmann[b], Thomas H. Helbich[c], Bernhard K. Keppler [a*]

[a] Institute of Inorganic Chemistry, University of Vienna, Waehringer Strasse 42, Vienna 1090, Austria

[b] Department of Environmental Geosciences, University of Vienna, Althanstrasse 14, Vienna 1090, Austria

[c] Department of Radiology, Medical University of Vienna, Waeringer Guertel 18-10, Vienna 1090, Austria

[*] Corresponding author. Tel: +43 1 4277 52602, Fax: +43 1 4277 52680, E-mail: bernhard.keppler@univie.ac.at

Abstract

Human serum albumin (HSA) derived nanoparticles represent promising systems for the development of diagnostic agents. Endothelial cell targeting lectins covalently conjugated to Gd-HSA combine magnetic resonance imaging (MRI) contrast enhancement with the advantages of tissue targeting. The present study reports the preparation of Gd(III) loaded albumin-lectin nanoparticles by different strategies for their potential exploration as targeted MRI contrast agents. As *in vivo* behaviour of nanoparticles strongly depends on particles dimension, the size as well as the polydispersity index has been evaluated for each preparation method. PCS measurements indicated a nanoparticles size range between 112 nm and 304 nm. Furthermore, the impact on the relaxation behaviour was determined by MRI experiments.

Introduction

Gadolinium based contrast agents have become a powerful imaging modality in magnetic resonance imaging (MRI). High spatial resolution images of soft tissues are provided by this non-invasive diagnostic technique (Caravan et al., 1999; Merbach and Toth, 2001). Nevertheless, free Gd(III) is known to be toxic and may cause damage to spleen, liver and bones and lead to nephrogenic systemic fibrosis (Sieber et al., 2008). Consequently, stable chelates are required. The use of polyaminocarboxylic acid ligands like the linear diethylenetriaminepentaacetic acid (DTPA), the macrocyclic 1,4,7,10-tetraazacyclododecane-*N,N',N'',N'''*-tetraacetic acid (DOTA) or backbone modified derivatives thereof prevent the release of free Gd(III) and hence reduce the risk of the mentioned side effects (Hermann et al., 2008).

However, the use of low molecular weight contrast agents is limited due to their rapid clearance and diffusion from the vasculature into the interstitial space (Barrett et al., 2006). The attachment of low molecular weight contrast agents to nanospheres presents auspicious possibilities for improved biophysical and pharmacological properties. Increased rotational correlation time for enhanced relaxvity per gadolinium atom and the prolonged intravascular retention - leading to the increase of molar relaxivities from the vasculature over an extended period of time - provide the main advantages. Such macromolecular contrast media may define a blood-tissue barrier comparable to the existing barrier for large molecular endogenous substances in the blood like plasma proteins (Brasch and Daldrup-Link, 2003).

The most common approaches for the preparation of contrast enhancing nanoparticles include the conjugation of Gd(III) chelates to dextrans (Sirlin et al., 2004), dendrimers (Langereis et al., 2006; Xu et al., 2007a; Xu et al., 2007b; Kido et

al., 2009), liposomes (Barrett et al., 2006), gold particles (Alric et al., 2008), polymers (Caravan et al., 1999) and albumins (Ogan et al., 1987; Barrett et al., 2006; Yan et al, 2006).

A remarkable perspective in MRI provides the introduction of a tissue specific targeting moiety to the contrast agent. High local concentration of contrast enhancing material at a particular site within the human body enables precise medical diagnosis and will become an essential tool in tracking the progress of therapies. Currently, great effort is invested in the development of such tissue specific contrast agents. The concept of liver targeting is realized by the introduction of lipophilic moieties to the contrast agent or alternatively, the encapsulation of Gd-DTPA or Gd-DOTA chelates into liposomal nanoparticles (Weinmann et al., 2003). Development of MRI contrast agents with the capability of seeking out tumors is approached by different strategies. One proposal is the non-covalent interaction of contrast agents bearing charged residues with charged groups of polyornithine and polyarginine. It is known, that positively charged polyaminoacids selectively bind to tumors as their charge is more negative than non-tumor cells (Aime et al., 2000). Receptor targeting through monoclonal antibodies attached to contrast enhancing molecules is also widely investigated in this field of research. Monoclonal antibodies are an important category of targeting vectors and can be prepared to interact with a variety of receptor sites (Jaques and Desreux, 2002). Recently, the preparation and investigation of a peptide targeted contrast agent for molecular magnetic resonance imaging of fibronectin-fibrin complexes in tumor tissues was published (Ye et al., 2008). The ability of imaging and diagnosing atherosclerotic plaques is of considerable interest since atherosclerotic diseases are among the leading causes of death in developed countries. Investigated methods to face the challenge of imaging fatty deposits

include the application of recombinant high density lipoprotein (HDL) like nanoparticles (Frias et al., 2004). Newly published investigations provide characterization of plaque in deep seated arteries using motexafin gadolinium (Brushett et al., 2008). MS 325, a gadolinium chelate that reversible binds to albumin in plasma has also been applied and areas of high signal intensity have been observed and were suggested not only to reflect the increased plaque vascularity but also the leakiness of the microvessels (Choudhury et al., 2002). In principle, also unspecific macromolecular or low molecular weight contrast agents suitable for imaging the blood pool bear the potential of indicating pathological alteration of the vasculature (Briley-Saebo et al., 2007).

A targeting group capable of binding to endothelial cells is the tomato derived lectin LEA (Lycopersicon esculentum agglutinin) (Porter et al., 1990; Mazzetti et al., 2004). The attachment of this lectin to gadolinium loaded nanoparticles has already shown to provide contrast media with the ability of imaging the blood vessel walls in high spatial resolution (Paschkunova-Martic et al., 2005).

Due to a considerably high number of functional groups albumin based nanoparticles represent promising systems for the development of MRI contrast enhancement and drug carriage facilities. Additionally, human serum albumin (HSA) derived nanospheres will be tolerated without side effects, since HSA is an integral component of plasma. The objective of this study was the preparation of Gd(III) loaded albumin-lectin nanoparticles for the exploration in targeted magnetic resonance imaging. For this purpose a bifunctional chelating agent was covalently attached to HSA and loaded with Gd(III). Different strategies were then explored to conjugate the modified albumin to LEA. Investigations of particle size and zeta

potential are also described. Finally, the relaxation behavior of the synthesized nanoparticles was evaluated.

Materials and methods

Chemicals and reagents

Human serum albumin, Lectin (from Lycopersicon esculentum), phosphate buffered saline (1×PBS), glutaric dialdehyde (50 wt.% solution in water), glutaric anhydride as well as citric acid trisodium salt dihydrate and citric acid monohydrate for buffer preparation were purchased from Sigma-Aldrich. *N*-(3-dimethylaminopropyl)-*N´*-ethyl-carbodiimide hydrochloride (EDC), 2-aminoethanol and sodium bicarbonate were obtained from Fluka. Ethanol (LiChrosolve®, gradient grade for liquid chromatography) was purchased from Merk. Trisodium bis(nitrilotriacetate)gadolinate solution ($Na_3[Gd(NTA)_2]$) (Paschkunova-Martic et al., 2005) as well as 2-(*para*-aminobenzyl)-diethylenetriaminepentaacetic acid tetrahydrochloride (NH_2-Bn-DTPA·4 HCl) (Cummins et al., 1991) were prepared according to literature procedures. All water used was purified by a Millipore Synergy 185 UV Ultrapure Water System (Molsheim, France).

Preparation of Gd(III) loaded human serum albumin

Conjugation of the bifunctional chelating agent and subsequent complexation with Gd(III) was performed using a method described in a previous manuscript in this thesis (Kundu et al. 2009). HSA (53 mg, 0.8×10^{-3} mmol) was dissolved in 0.1 M $NaHCO_3$ (10 ml) and cooled to 4°C. Glutaric anhydride (62 mg, 543.4×10^{-3} mmol) was added slowly in small portions while the pH of the mixture was maintained within a range of 7.8 - 8.2 by the addition of 0.6 M NaOH. Afterwards, the solution was stirred for 22 h at 4°C. To remove excess reagents the albumin-solution was

concentrated by centrifugation (Vivaspin 20, MWCO: 30000, 2500×g, 19°C) and washed with water (three times). The purified glutarylated albumin solution was diluted with H_2O (7 ml) and NH_2-Bn-DTPA•4HCl (60 mg, 931×10^{-3} mmol) in H_2O (2 ml) were added at ambient temperature. During the addition, the pH was repeatedly adjusted to 6.8 - 7.2 by 0.3 M NaOH. EDC (8 mg) was added and the conjugation reaction proceeded for 2 h at room temperature. To separate non-conjugated bifunctional ligand and low molecular weight compounds the solution was concentrated by centrifugation (Vivaspin 20, MWCO: 30000, 2500×g, 19°C) and again washed with water (three times). For the purpose of complexation with Gd(III) the modified albumin was then dissolved in 0.1 M citric buffer (10 ml) (pH 6.5) and cooled to 4°C. 0.1 M $Gd(NTA)_2$ solution (2.5 ml, 0.25 mmol) was added and allowed to react for 19 h. Finally, the reaction mixture was concentrated by centrifugation (Vivaspin 20, MWCO: 30000, 2500×g, 19°C) and washed with water (three times) to give a purified aqueous solution (10 mg/ml) of the gadolinium loaded HSA.

Albumin determination

The protein concentration of purified gadolinium loaded albumin solutions was determined by the method of Bradford. A Bradford test kit from Bio-Rad Laboratories (Vienna, Austria) was used and adapted for usage in 96 - well plates. Optical densities at 595 nm were recorded on a microplate reader (Synergy HT, Biotek) 15 min. after the addition of Bradford solution.

Determination of the gadolinium content

Gadolinium content of purified loaded albumin solutions was determined by an ICP-MS (Inductively Coupled Plasma Mass Spectrometry) instrument (Agilent 7500ce, Waldbronn, Germany), equipped with a CETAC ASX-520 autosampler (Neuss, Germany), a Scott double pass spray chamber, and a MicroMist nebulizer.

Preparation of Gd-HSA-Lectin nanoparticles by the activation of HSA (method 1)

Gd-HSA solution (0.531 ml, 5.31 mg) was diluted in PBS (1 ml) and the pH was adjusted to 8 by the use of 0.01 M NaOH. Glutaraldehyde ((10 µl, 10% solution) was added and mixed by rotation (Multi Bio RS 24) for 5 h at 30 rpm. To remove excess glutaraldehyde the reaction liquid was concentrated by centrifugation (Vivaspin 20, MWCO: 30000, 2500×g, 19°C) and washed with water (three times). The activated Gd-albumin was diluted in PBS (3 ml) and LEA (2 mg) dissolved in H_2O (0.4 ml) was added. After 18 h of rotation (Multi Bio RS 24) at 30 rpm the reaction was quenched by the addition of aminoethanol (20 µl) and the suspension was rotated for one further hour. The resulting nanoparticles were purified by centrifugation (Vivaspin 20, MWCO: 30000, 2500×g, 19°C) and redispersion in water (three times).

Preparation of Gd-HSA-Lectin nanoparticles by desolvation (method 2)

The nanoparticles were prepared using a modification of a previously described technique (Weber et al., 2000; Langer et al., 2003). Gd-HSA solution (0.53 ml, 5.31 mg) was diluted in H_2O (1 ml) and LEA (2 mg) dissolved in H_2O (0.4 ml) was added. The pH was adjusted to 8.2 with 0.01 M NaOH. EtOH (1.6 ml) was added dropwise

(1 ml/min) under constant stirring (1000 rpm) at room temperature. Subsequently, glutaraldehyde (8 µl, 10% solution) was added to crosslink the protein molecules. The reaction proceeded for 22 h under stirring. Unconverted glutaraldehyde was inactivated by the addition of aminoethanol (20 µl) and the suspension was stirred for a further hour. The resulting nanoparticles were purified by centrifugation (Vivaspin 20, MWCO: 30000, 2500×g, 19°C) and redispersion in water (three times).

Preparation of Gd-HSA-Lectin nanoparticles by simultaneous crosslinking (method 3)

At room temperature, Gd-HSA solution (0.53 ml, 5.31 mg) was diluted in H_2O (1 ml) and LEA (2 mg) dissolved in H_2O (0.4 ml) was added. The pH was adjusted to 8.2 with 0.01 M NaOH. To start the crosslinking reaction glutaraldehyde (8 µl, 10% solution) was added and the reaction was allowed to proceed for 22 h. Excess glutaraldehyde was inactivated by the addition of aminoethanol (20 µl) and the suspension was stirred for a further hour. The resulting nanoparticles were purified by centrifugation (Vivaspin 20, MWCO: 30000, 2500×g, 19°C) and redispersion in water (three times).

Preparation of Gd-HSA-Lectin nanoparticles by the activation of LEA (method 4)

LEA (2.5 mg) dissolved in H_2O (0.5 ml) was diluted in 0.1 M $NaHCO_3$ (4 ml) and cooled to 4°C. Glutaric anhydride (15 mg) was added in small portions and the pH was maintained between 7.8 and 8.2 by the addition of 0.1 M NaOH. The glutarylation was allowed to proceed for 2 h at 4°C. Thereafter, repeated centrifugation (Vivaspin 20, MWCO: 30000, 2500×g, 19°C) and washing with water

removed small molecular weight compounds. The purified and concentrated glutarylated lectin solution was diluted with water (7 ml). Gd-HSA solution (0.7 ml, 7 mg) was added and the pH was adjusted to 6.7 by 0.1 M HCl. EDC (5 mg) was added and the conjugation reaction proceeded for 1 h. During this time the pH was permanently corrected to 6.7. The resulting nanoparticles were purified by centrifugation (Vivaspin 20, MWCO: 30000, 2500×g, 19°C) and redispersion in water (three times).

Measurement of particle size and zetapotential

Particle size distribution of the undiluted sample was measured by dynamic light scattering (DLS) at a 173° angle using a Zetasizer Nano ZS (Malvern Instruments, UK). Each measurement consists of 5 runs of 20 sec. The temperature of the dispersant (ultrapure water) was set to 21 °C. We used low volume disposable sizing cuvettes made from poly methyl metacrylate.

In a first step the measured autocorrelation function was analyzed by the cumulant method with quadratic weighing for the average particle size (z-average, first cumulant) and the polydispersivity (PDI, second cumulant). For particle size distribution analysis we used in addition the Malvern Instruments general purpose method, i.e. a fitting of the autocorrelation function to a set of logarithmic decay functions. We used the mode (i.e. the 1st peak of the intensity weighted distribution) for further data interpretation. Especially for broader particle size distributions with a higher polydispersivity the z-average determined by the cumulant anlysis differs from the mode determined by the general purpose method.

The electrophoretic mobility of the particles was measured by laser Doppler velocimetry with the same instrument. We used folded capillary cells and injected the undiluted samples with a syringe to prevent encapsulation of air bubbles. The Smoluchowski approximation (F(*Ka*) = 1.5) was used to calculate the zeta potential from electrophoretic mobility. We calculated average values and standard deviation out of three individual measurements.

Spin-Lattice and Spin-Spin Relaxivity measurements

Relaxivity measurements were performed on a 3 Tesla whole-body MRI scanner (TimTrio 3 T, Siemens Medical Solutions, Erlangen, Germany) using a whole body coil for excitation and standard head receiver coil for signal reception. Homogeneity of B_1-field was insured by test measurements before the actual measurements of relaxivity. For each agent four dilutions ranging from 1.25 mg/ml to 10 mg/ml in PBS with the volume of 0.25 ml were prepared. All probes were measured in standard PE-tubes with a diameter of 0.8 cm. The tubes were placed in the centre of a plastic box surrounded by water heated to 37°C.

For the determination of spin-lattice relaxation times T_1, spin echo inversion recovery (IR) sequences with inversion times from 0 to 3500 ms (TI = 0, 60, 80, 100, 150, 200, 250, 300, 400, 500, 750, 1000, 1250, 1500, 1750, 2000, 2500, 3500 ms) were used. An adiabatic pulse was applied for B1 insensitive inversion. The other parameters were: TR/TE = 5000/8.1 ms; flip angle 180°; 8 turbo factor 11; FOV read 180 × 180 mm; resolution matrix 192 × 192; bandwidth 260 Hz/pixel; and slice thickness 3 mm. The mean values of the signal intensities, the standard deviations, and pixel counts were determined by drawing regions of interest. The area assessed measured

between 0.12 cm^2 and 0.14 cm^2; for each measurement series, the measured area was kept identical by copying and pasting the ROI. For all measurements, the relaxation rates (R_1) and the relaxivities (r_1) were calculated for each substance. The longitudinal relaxation rate (R_1) was calculated using the equation:

$$SI(TI) = A[1-2\exp(-R_1*TI)+\exp(-R_1*TR)] \quad [1]$$

with SI being the signal intensity as a function of TI, "A" accounting for the thermal equilibrium magnetization M0, and TI being the inversion time in ms.

For the determination of individual spin-spin relaxation times (T_2), spin-echo sequence with multiple echoes (NE= 5) ranging from 13.8 ms to 69 ms was used. Repetition time was set to 2500 ms, FOV 160 × 160 mm, resolution matrix 128 × 128, bandwidth 260 Hz/pixel; and slice thickness 3 mm. The mean values of the signal intensities, the standard deviations, and pixel counts were determined by drawing regions of interest. The area assessed measured between 0.12 cm^2 and 0.14 cm^2; for each measurement series, the measured area was kept identical by copying and pasting the ROI. For all measurements, the relaxation rates (R_2) and the relaxivities (r_2) were calculated for each substance. The transversal relaxation rates (R_2) were calculated as the reciprocal value of the slope of semilogarithmic plot of signal intesities at individual echo times and respective echo times.

The relaxivities (r_1, r_2) were calculated as the slope of linear regression of R_1 and R_2 as a function of contrast agent concentration.

Results and Discussion

The objective of this study was the evaluation of different parameters to characterize the prepared nanoparticles with regard to a possible application in MRI.

The synthesis of Gd(III) loaded human serum albumin is based on a technique described in a previous manuscript in this thesis (Kundu et al., 2009). The bifunctional chelating agent NH_2-Bn-DTPA was covalently attached to the albumin by a glutaric acid linker. Amide coupling to the primary amine functionalities of lysine residues as well as amide formation to the primary amine of the ligand provided stable conjugation. Gadolinium coordination exclusively to the DTPA derivative succeeded by the introduction of a $Gd(NTA)_2$ solution. Nitrilotriacetic acid was utilized for the reason of being a weak ligand for Gd(III) and therefore, to prevent nonspecific complexation to proteins which may result in the release of free Gd(III) (Spanoghe et al., 1992). The gadolinium:albumin ratio was determined by the measurement of protein concentration by the Bradford assay and the determination of the metal content by ICP-MS. The detected gadolinium amount was related to the protein concentration and indicated that 35 contrast enhancing Gd(III) ions were attached to each albumin molecule (Figure 1).

Syntheses of nanoparticles were performed by four different strategies to indicate possible variations in size, zeta potential and relaxivity behavior. The homobifunctional reagent glutaraldehyde was chosen as crosscoupling reagent due to its convenient handling. The use of this probably most popular protein crosslinking reagent is well established in literature (Hermanson, 2008). After the reaction, remaining aldehyde functionalities were inactivated by the addition of aminoethanol. This procedure prevented further crosscoupling. Applied techniques covered the

activation of Gd-HSA with glutaric dialdehyde followed by subsequent addition of the lectin for conjugation (method 1). Furthermore, a preparation method utilizing a modification of a previously described desolvation technique (Weber et al., 2000; Langer et al., 2003) has been investigated (method 2). The simultaneous crosslinking of Gd-HSA and LEA by glutaraldehyde was examined as well (method 3). Finally, the crosslinking of Gd-HSA and LEA with prior activation of the lectin by glutaric anhydride has been performed (method 4). The choice of employing glutaric anhydride was made to evaluate possible differences in size or size distribution in contrast to nanoparticles derived from glutaraldehyde crosslinking.

The particle size distribution of nanoparticles prepared by all four methods show multiple peaks. The first peak is mostly attributable to unconverted starting material (at around 10 nm). None of the methods described did completely polymerize the provided Gd-HSA and lectin molecules. A discrimination of Gd-HSA and LEA by PCS is not possible as both have almost the same size. The high intensities of unpolymerized material do not necessarily indicate a higher amount of not conjugated proteins in comparison to crosslinked nanoparticles. The second peak indicates the polymerized Gd-loaded nanoparticles. Method 4 produced the smallest particles (112 nm) compared to the other methods (186 to 304 nm). This might be a consequence of the applied method of synthesis. Primary activation of LEA and subsequent conjugation to Gd-HSA through a glutaric acid linker give well defined structures of nanoparticles. This is also indicated by the low PDI (0.19). In contrast, preparation method 1-3 – conjugated by glutaraldehyde linkage - form Gd-HSA-LEA conjugates having increased size and a less narrow size distribution and higher PDI, indicating the heterogeneity of the sample (see also Table 1). These differences can possibly be explained by the distinct properties of the linkers. Glutaric acid, bearing

two acid functionalities, connects two macromolecules. Whereas, it is known that glutaraldehyde forms *α,β* - unsaturated polymers in aqueous solutions which are highly reactive towards primary amines. The polymer size and structure is unknown and may be influenced by the age of the glutaraldehyde solution (Hermanson, 2008). As the glutaraldehyde polymer provides more than just two reactive functionalities per molecule, it promotes further crosslinking leading to a broader distribution of formed nanoparticles. However, method 4 also shows a distinct peak at 463 nm which can be interpreted as a temporary reversible aggregation. Peaks above 1 µm can be interpreted as remnants of the autocorrelation fitting algorithm or, although unlikely, as contamination through dust.

The ability of the Gd-HSA-LEA conjugates to modify the relaxation rate of water was evaluated at 37°C in PBS. Relaxation rates (R_1, R_2) and respective relaxivities (r_1, r_2) were measured at 3T and are displayed in Table 2. As the accurate structure and molecular weight of the tomatoe lectin is still unclear (Oguri et al., 2008), the molecular weight of the prepared nanoparticles is hardly to determine. For that reason the relaxation rates and the relaxivities are given related to the amount of substance in mg. Two effects account for the differences in relaxivity. First, accessibility of the gadolinium ion for protons within the Gd-HSA-LEA conjugates prepared by diverse techniques and secondly, the variations in the tumbling rate of the nanoparticles. These properties impact the water exchange rate and hence, the relaxivity of the particles.

In conclusion, Gd-HSA-LEA nanoparticles were prepared by four different strategies. Particle size measurement indicated a range between 112 and 304 nm depending on the preparation method. Additionally, the relaxation behavior was evaluated. In effort to develop contrast agents with the capability of targeting the vasculature, further

investigations on the *in vivo* behavior like chelate stability, the degradability and the accumulation of these contrast enhancing conjugates at endothelial cells are required.

Figures and Tables

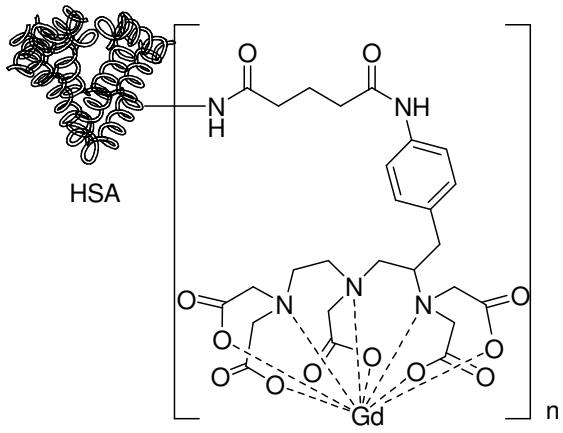

n= 35

Figure 1. Gd(III) loaded HSA.

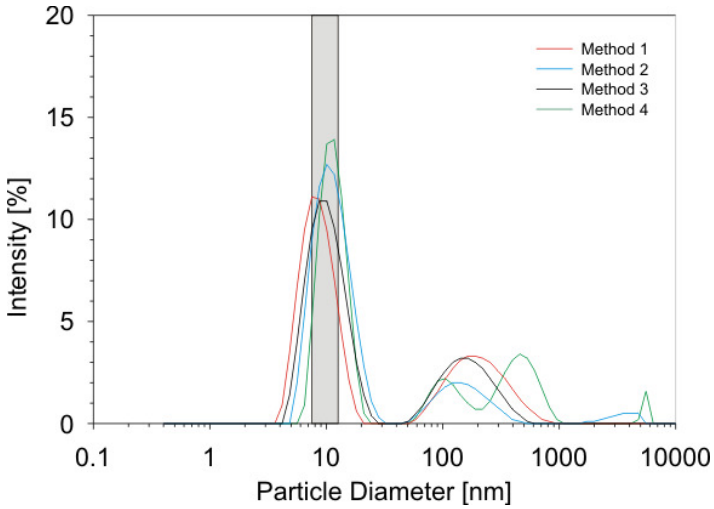

Figure 2. Particle size distribution (nm) by intensity (%) for nanoparticle synthesis method 1 to 4 as well as the range for Lectin (grey bar).

Table 1. Detailed characterization of synthesized nanoparticles by dynamic light scattering (n=3, ± 1SD).

	z-average (nm)	peak 1 (nm) ± 1SD	peak 2 (nm) ± 1SD	peak 3 (nm) ± 1SD	PDI	Count rate (kcps)	Zeta potential (mV) ± 1SD
Method 1	11.8	11.8 ± 3.82	304 ± 172.6	-	0.61	114.9	-0.69 ± 0.03
Method 2	12.2	13.5 ± 4.79	186 ± 90.10	4090 ± 53	0.59	144.4	-0.32 ± 0.19
Method 3	13.6	14.0 ± 5.02	239 ± 121.3	-	0.65	185.9	-2.39 ± 0.36
Method 4	95.9	11.6 ± 2.88	112 ± 33.6	463 ± 162.2	0.19	151.8	1.24 ± 0.4
LEA	1842.0	15.7 ± 1.50	-	-	1.00	387.8	-

Table 2. Relaxation behavior of the nanoparticles

Method	$c_{conjugate}$(mg/ml)	$R_1(s^{-1})$	$r_1[s^{-1}*(mg/ml)^{-1}]$	$R_2(s^{-1})$	$r_2[s^{-1}*(mg/ml)^{-1}]$
Method 1	10	2.414	0.166	4.097	0.284
	5	1.669		2.989	
	2.5	1.389		2.350	
	1.25	0.826		1.389	
Method 2	10	4.108	0.354	8.130	0.686
	5	/		/	
	2.5	1.591		3.210	
	1.25	1.047		1.980	
Method 3	10	3.688	0.294	7.515	0.607
	5	3.044		6.295	
	2.5	1.699		3.431	
	1.25	1.053		2.964	
Method 4	10	4.902	0.445	11.336	1.023
	5	3.032		7.307	
	2.5	1.680		4.082	
	1.25	0.972		2.21	

References

Aime, S., Botta, M., Garino, E., Crich, S. G., Giovenzana, G., Pagliarin, R., Palmisano, G., Sisti, M., 2000. Non-covalent Conjugates between Cationic Polyamino Acids and Gd (III) Chelates: A Route for Seeking Accumulation of MRI-Contrast Agents at Tumor Targeting Sites. Chem. Eur. J., 6, 2609-2617.

Alric, C., Taleb, J., Le Duc, G., Mandon, C., Billotey, C., Le Meur-Herland, A., Brochard, T., Vocanson, F., Janier, M., Perriat, P., Roux, S., Tillemant, O., 2008. Gadolinium Chelate Coated Gold Nanoparticles As Contrast Agents for Both X-ray Computed Tomography and Magnetic Resonance Imaging. J. Am. Chem. Soc., 130, 5908-5915.

Barrett, T., Kobayashi, H., Brechbiel, M., Choyke, P. L., 2006. Macromolecular MRI contrast agents for imaging of tumor angiogenesis. Eur. J. Radiol., 60, 353-356.

Brasch, R. C., Daldrup-Link, H. E., 2003. Macromolecular contrast agents for MR mammography: current status. Eur. Radiol. 13, 354-365.

Briley-Saebo, K. C., Mulder, W. J. M., Mani, V., Hyafil, F., Amirbekian, V., Aguinaldo, J. G. S., Fisher, E. A., Fayad, Z. A., 2007. Magnetic Resonance Imaging of Vulnerable Atherosclerotic Plaques: Current Imaging Strategies and Molecular Imaging Probes. J. Magn. Reson. Imaging, 26, 460-479.

Brushett, C., Qiu, B., Atalar, E., Yang, X., 2008. High Resolution MRI of Deep Seated Atherosclerotic Arteries Using Motexafin Gadolinium. J. Magn. Reson. Imaging, 27, 246-250.

Caravan, P., Ellison, J. J., McMurry, T. J., Lauffer, R. B., 1999. Gadolinium (III) Chelates as MRI Contrast Agents: Structure, Dynamics, and Applications. Chem. Rev., 99, 2293-2352.

Choudhury, R. P., Fuster, V., Badimon, J. J., Fisher, E. A., Fayad, Z. A., 2002. MRI and Characterization of Atherosclerotic Plaque: Emerging Applications and Molecular Imaging. Arterioscler. Thromb. Vasc. Biol., 22, 1065-1074.

Cummins, C. H., Rutter, E. W., Fordyce, W. A., 1991. A Convenient Synthesis of Bifunctional Chelating Agents Based on Diethylenetriaminepentaacetic Acid and their Coordination Chemistry with Yttrium (III). Bioconjugate Chem. 2, 180-186.

Frias, J. C., Williams, K. J., Fisher, E. A., Fayad, Z. A., 2004. Recombinant HDL-Like Nanoparticles: A Specific Contrast Agent for MRI of Atherosclerotic Plaques. J. Am. Chem. Soc., 126, 16316-16317.

Hermann, P., Kotek, J., Kubíček, V., Lukeš, I., 2008. Gadolinium (III) complexes as MRI contrast agents: ligand design and properties of the complexes. Dalton Trans., 3027-3047.

Hermanson, G. T., 2008. Bioconjugate Techniques. 2nd Edition. Elsevier

Jaques, V., Desreux, J. F., 2002. New Classes of MRI Contrast Agents. Topics In Current Chemistry, 221, 123.164.

Kido, N., Xu, H., Regino, C. A. S., Bernardo, M., Ileva, L., Riffle, L., Wong, K. J., Brechbiel, M. W., 2009. A New Approach in the Preparation of Dendrimer-Based Bifunctional Diethylenetriaminepentaacetic Acid MR Contrast Agent Derivatives. Bioconjugate Chem., 20, 1412-1418.

Kundu, A., Peterlik, H., Krssak, M., Bytzek, A. K., Helbich, T. H., Keppler, B. K., 2009. Strategies for the covalent conjugation of a bifunctional chelating agent to albumin: synthesis and characterization of potential MRI contrast agents. (in preparation)

Langer, K., Balthasar, S., Vogel, V., Dinauer, N., von Briesen, H., Schubert, D., 2003. Optimization of the preparation process for human serum albumin (HSA) nanoparticles. Int. J. Pharm., 257, 169-180.

Langereis, S., de Lussanet, Q. G., van Genderen, M. H., Meijer, E. W., Beets-Tan, R. G., Griffioen, A. W., van Engelshoven, J. M., Backes, W. H., 2006. Evaluation of Gd (III) DTPA-terminated poly(propylene imine) dendrimers as contrast agents for MR imaging. NMR Biomed., 19, 133-141.

Mazzetti, S., Frigerio, S., Gelati, M., Salmaggi, A., Vitellaro-Zuccarello, L., 2004. Lycopersicon esculentum lectin: an effective and versatile endothelial marker of normal and tumoral blood vessels in the central nervous system. Eur. J. Histochem., 48, 423-428.

Merbach, A. E., Tóth, É., 2001. The Chemistry of Contrast Agents in Medical Magnetic Resonance Imaging. John Wiley & Sons, New York

Ogan, M. D., Schmiedl, U., Moseley, M. E., Grodd, W., Paanjanen, H., Brasch, R. C., 1987. Albumin labeled with Gd-DTPA. An intravascular contrast enhancing agent for magnetic resonance blood pool imaging: preparation and characterization. Invest. Radiol., 22, 665-671.

Oguri, S., Amano, K., Nakashita, H., Nagata, Y., Momonoki, Y. S., 2008. Molecular Structure and Properties of Lectin from Tomato Fruits. Biosci. Biotechnol. Biochem., 72, 2640-2650.

Paschkunova-Martic, I., Kremser, C., Mistlberger, K., Shcherbakova, N., Dietrich, H., Talasz, H., Zou, Y., Hugl, B., Galanski, M., Sölder E., Pfaller, K., Höliner, I., Buchberger, W., Keppler, B., Debbage, P., 2005. Design, synthesis, physical and chemical characterisation, and biological interactions of lectin-targeted latex nanoparticles bearing Gd-DTPA chelates: an exploration of magnetic resonance molecular imaging (MRMI). Histochem. Cell Biol., 123, 283-301.

Porter, G. A., Palade, G. E., Milici, A. J., 1990. Differential binding of the lectins Griffonia simplicifolia I and Lycopersicon esculentum to microvascular endothelium: organ-specific localization and partial glycoprotein characterization. Eur. J. Cell Biol., 51, 85-95.

Sieber, M.A., Pietsch, H., Walter, J., Haider, W., Frenzel, T:, Weinmann, H. J., 2008. A Preclinical Study to Investigate the Development of Nephrogenic Systemic Fibrosis: A Possible Role for Gadolinium-Based Contrast Media. Invest. Radiol., 43, 65-75.

Sirlin, C. B., Vera, D. R., Corbeil, J. A., Caballero, M. B., Buxton, R. B., Mattrey, R. F., 2004. Gadolinium-DTPA-dextran: a macromolecular MR blood pool contrast agent. Acad. Radiol., 11, 1361-1369.

Spanoghe, M., Lanens, D., Dommisse, R., Van der Linden, A., Alderweireldt, F., 1992. Proton Relaxation Enhancement By Means of Serum Albumin And Poly-L-Lysine Labeled With

DTPA-Gd^{3+}: Relaxivities As A Function Of Molecular Weight And Conjugation Efficiency. MagneticResonance Imaging, 10, 913-917.

Weber, C., Kreuter, J., Langer, K., 2000. Desolvation process and surface characteristics of HSA-nanoparticles. Int. J. Pharm. 196, 197-200.

Weinmann, H. J., Ebert, W., Misselwitz, B., Schmitt-Willich, H., 2003. Tissue-specific MRI contrast agents. Eur. J. Radiol., 46, 33-44.

Xu, H., Regino, C. A. S., Bernardo, M., Koyama, Y., Kobayashi, H., Choyke, P. L., Brechbiel, M. W., 2007a. Towards Improved Syntheses of Dendrimer-Based Magnetic Resonance Imaging Contrast Agents: New Bifunctional Diethylenetriaminepentaacetic Acid Ligands and Nonaqueous Conjugation Chemistry. J. Med. Chem., 50, 3185-3193.

Xu, H., Regino, C. A. S., Koyama, Y., Hama, Y., Gunn, A. J., Bernardo, M., Kobayashi, H., Choyke, P. L., Brechbiel, M. W., 2007b. Preparation and preliminary evaluation of a biotin-targeted, lectin-targeted dendrimer-based probe for dual modality magnetic resonance and fluorescence imaging. Bioconjugate Chem., 18, 1474–1482.

Yan, G. P., Robinson, L., Hogg, P., 2007. Magnetic resonance imaging contrast agents: Overview and perspectives. Radiography, 13, 5-19.

Ye, F., Jeong, E. K., Jia, Z., Yang, T., Parker, D., Lu, Z. R., 2008. A Peptide Targeted Contrast Agent Specific to Fibrin-Fibronectin Complexes for Cancer Molecular Imaging with MRI. Bioconjugate Chem., 19, 2300-2303.

Curriculum vitae

Dipl. Ing. Amitava Kundu

Rudolf Nurejew Promenade 1/8/10

1220 Wien

Tel.: 0650 5116117

Email: amitava.kundu@univie.ac.at

Personal data

Date of birth:	May 26th 1975
Place of birth:	Berlin
Nationality:	German

Education

since 2007	Ph.D. Research at the Institute of Inorganic Chemistry at the **University of Vienna** title: *Development and Optimization of Multifunctional Nanoparticles for Molecular Imaging*
1997 – 2006	Studies of Technical Chemistry at the **Vienna University of Technology**
1994 – 1997	Studies of Medicine (5 semesters) at the **University of Vienna**
1985 – 1994	Gymnasium
1981 – 1985	Elementary school

Traineeship

September 1999	practical training: Laboratory for lubricants (**OMV**)
February 1999	practical training: Institute for Petroleum Research **FICHTE (ARC Seibersdorf)**
September 1998	practical training: Institute for Petroleum Research **FICHTE (ARC Seibersdorf)**

Further activities

2008 – 2009	Lector at the Institute of Inorganic Chemistry, **University of Vienna**
2009	Tutor at the Institute of Inorganic Chemistry, **University of Vienna**
July 2007	Participation at the **13th International Conference on Biological Inorganic Chemistry** (ICBIC)
September 2003	Participation at the **10th Blue Danube Symposium on Heterocyclic Chemistry** (BDSHC)
2001 – 2002	Participation on the preparation of electronical, chemical textbooks (**Vienna University of Technology**)
2000 – 2002	Project management, Flash programming at **Create-Mediadesign**

Computer literacy

MS Office, ChemDraw, Isis Draw, WinNMR, WinIR, Beilstein Commander, Sci-Finder

Language skills

English: fluent in spoken and written

French: school knowledge

Spanish: basics

Scientific publication

Peter Gärtner and Amitava Kundu

"Chiral Auxiliaries on Solid Support"

in: *"The Power of Functional Resins in Organic Synthesis"*, F. Albericio and J. Pulla-Tuche (eds.); Wiley-VCH, Weinheim, 2008, 329 – 363

Reports

A. Kundu, B.K. Keppler

„Nanopartikel zur Diagnose von Blutgefäßerkrankungen";

Nachrichten aus der Chemie, **55**, 9, (2007), 842-846

A. Kundu

„Bioanorganiker in Wien" (Tagungsbericht zur 13. ICBIC)

Nachrichten aus der Chemie, **55**, 10, (2007), 1036